COMMUNICATION SCIENCES

AND

ENGINEERING

XVII. STATISTICAL COMMUNICATION THEORY*

Prof. Y. W. Lee	R. Alter	L. Goodman
Prof. A. G. Bose	M. Austin	S. Greenblatt
Prof. M. Schetzen	A. B. Baggeroer	T. Kincaid
Prof. H. L. Van Trees	R. F. Bauer	D. Kurtz
Prof. V. R. Algazi	A. M. Bush	D. E. Nelsen
Prof. J. D. Bruce	L. D. Collins	R. Parente
Prof. A. V. Oppenheim	T. Froeschle	D. Snyder

RESEARCH OBJECTIVES AND SUMMARY OF RESEARCH

This group is interested in various aspects of statistical communication theory with particular emphasis on nonlinear systems and noise. A special field of investigation is that of two-state modulation. Current research problems are: (1) Application of generalized superposition theory to nonlinear filtering, (2) Studies in optimum quantization, (3) Filter performance, (4) Efficient techniques for the synthesis of nonlinear systems, (5) Analysis of nonlinear systems, (6) Coupled oscillators, (7) Analysis of commutator machines with random inputs by Volterra functionals, (8) Study of nonlinear systems through Kolmogorov partial differential equations, (9) Two-state circuitry problems, (10) Noise in two-state systems, and (11) Magnetic tape noise.

1. A theory of generalized superposition which represents an application of linear algebra to the treatment of nonlinear systems was presented by A. V. Oppenheim in 1964.[1,2] The proposed research is directed toward applying this theory to nonlinear filtering. In particular, the theory suggests an approach to signal design and filtering in time-variant and multipath communications channels. Also, this research will be concerned with a study leading to a generalization of the matched filter, the filter being in general a nonlinear homomorphic system whose class is specified by the manner in which signal and noise are combined in the channel.

2. In his research on optimum quantization, J. D. Bruce[3,4] has derived an exact expression for the quantization error as a function of the parameters that define the quantizer, the error-weighting function, and the amplitude probability density of the quantizer-input signal. An algorithm that permits the determination of the specific values of the quantizer parameters that define the optimum quantizer has been developed. This algorithm, which is based on a modified form of dynamic programming, is valid for both convex and nonconvex error-weighting functions. Furthermore, this error expression and this algorithm have been extended to the case for which the quantizer-input signal is a message signal contaminated by a noise signal. (The contamination is not required to be additive and the noise signal is not required to be independent of the message signal.) Recent progress in this research is described in this quarterly report.

3. V. R. Algazi[5] has reported on a study of the message characteristics that lead to good or poor separation from noise by linear and nonlinear filters. His work leads to the determination of lower bounds on the filtering error for various classes of messages. This research is a new approach to filtering which is related to the work of Balakrishnan and Tung. It circumvents the unrealistic requirement of knowing higher order statistics of the input, and tries to find qualitative reasons for the separability of messages in a background of noise. The work has progressed beyond the results reported in Technical Report 420, Research Laboratory of Electronics, M. I. T., June 27, 1964, to include the case of filters with memory.

4. Functional analysis of nonlinear systems has proved to be a useful tool for the analysis of a wide class of nonlinear systems. Systems of this class are characterized

*This work was supported in part by the National Science Foundation (Grant GP-2495), the National Institutes of Health (Grant MH-04737-04), and in part by the National Aeronautics and Space Administration (Grant NsG-496).

by a set of kernels. Methods of efficiently synthesizing a system from its description by a set of kernels are desirable from both practical and theoretical viewpoints. This research is a study of such synthesis procedures. The time-domain approach will be emphasized, and bandlimited systems and systems with sampled inputs and/or outputs will be studied. A. M. Bush reports a part of this research in this quarterly report.

5. A study of methods of analysis for nonlinear systems is proposed. It consists of two aspects. One is the study of various characterizations of nonlinear systems and of their advantages and disadvantages for different applications. The other aspect of this research is the development of practical techniques for determining the parameters of a given characterization.

6. Many physical processes can be phenomenologically described in terms of a large number of interacting oscillators. An example is an electric power-supply system for a city. It is known that the stability of many systems of coupled oscillators is better than that of any of the individual oscillators of which it is composed. This improvement in stability is due to the nonlinear interaction of the oscillators. A theoretical model has been devised which may be applicable to the study of such systems. Experimental work is being performed to establish physical correspondence of actual systems to this model. In the present phase of this study, the spectrum of a sinusoidal that is phase-modulated by a random wave is being investigated. The case in which the random wave is a Gaussian process has been studied. Experimental measurements for the case in which the random wave is a quadratic and the case in which the random wave is a cubic function of a Gaussian process are now being made.

7. The response of either a shunt of a series-wound commutator machine to its input voltage is described by a set of nonlinear differential equations. Solutions of these equations in the form of a Volterra functional series upon the input have been obtained. These solutions permit a new analysis of the behavior of these machines. Specifically, while the computation of the response of such machines to stochastic inputs is all but impossible to accomplish from their differential equation description, these computations have been obtained from their Volterra series description. A part of this study is reported by R. B. Parente in this quarterly report.

8. The first-order probability density associated with the response of a wide class of nonlinear systems to Gaussian random processes satisfies the forward and backward Kolmogorov partial differential equations. Also, averages, passage probabilities and other functions of the response satisfy the equations. The study of nonlinear systems through the Kolmogorov equations is possible in all regions of operation, and is therefore applicable when other methods such as linearization techniques fail. In many cases of interest, however, the equations are too formidable for exact solution. The initial purpose of the proposed research is to develop efficient computer solutions to the equations.

9. T. A. Froeschle has developed two threshold detecting devices with very small hysteresis, based on the work of A. G. Bose, and a highly flexibly two-state modulator for laboratory use. He has also investigated high-power switching circuits and devices. The results will be reported in his S. M. thesis.

10. An investigation is proposed that is concerned with evaluating noise in certain kinds of two-state systems. The two-state systems of interest are ones in which a continuous input signal is converted to two-state form by a suitable modulator (such as pulsewidth, pulse frequency, etc.). The modulator output is passed through a transmission channel, the output of which is processed by a receiver that attempts to recover the desired modulating signal. Besides possible distortion, which is characteristic of the modulation method used, the desired signal may be corrupted by noise arising in the modulator, the transmission channel or in the receiver. We are particularly interested in finding ways of evaluating the noise that originates in the circuit elements and devices comprising various parts of the system. A part of this work has been reported by D. E. Nelsen.[6]

11. A study is being made on the corruption, by noise, of a signal recorded on magnetic tape. This study was instigated by practical necessity when the problem of small signal-to-noise ratios began to plague us in projects requiring direct recording of wide-bandwidth signals. This signal-to-noise ratio is only 20-30 db, as specified by manufacturers of instrumentation recorders. Besides this practical stimulus, the project has taken on great theoretical interest because of an unusual characteristic of the noise; it is of two types. The first is the ordinary, independent noise component which is added to the signal, while the second noise component is dependent on the magnitude of the recorded signal. This second type of noise is called modulation noise or multiplicative noise. The primary concern of our investigation is the noise caused by the random variations in the magnetic characteristics of the tape. The goal of the study is to relate this noise to the physical properties (i.e., dipole moment, density, arrangement, orientation) of the magnetic particles composing the magnetic surface of the tape. R. F. Bauer reports progress on this study in this quarterly report.

Y. W. Lee

References

1. A. V. Oppenheim, Generalized superposition, Quarterly Progress Report No. 72, Research Laboratory of Electronics, M.I.T., January 15, 1964, pp. 176-183.

2. A. V. Oppenheim, Superposition in a Class of Nonlinear Systems, IEEE International Convention Record, Part I, March 1964, pp. 171-177.

3. J. D. Bruce, An Investigation of Optimum Quantization, Sc.D. Thesis, Department of Electrical Engineering, M.I.T., June 1964.

4. J. D. Bruce, On the Optimum Quantization of Stationary Signals, IEEE International Convention Record, Part I, March 1964, pp. 118-124.

5. V. R. Algazi, A Study of the Performance of Linear and Nonlinear Filters, Technical Report 420, Research Laboratory of Electronics, M.I.T., June 22, 1964.

6. D. E. Nelsen, Calculation of power density spectra for a class of randomly jittered waveforms, Quarterly Progress Report No. 74, Research Laboratory of Electronics, M.I.T., July 15, 1964, pp. 168-179.

A. KERNELS REALIZABLE EXACTLY WITH A FINITE NUMBER OF LINEAR SYSTEMS AND MULTIPLIERS

Schetzen[1] has discussed the synthesis of second-degree nonlinear systems using a finite number of linear systems and multipliers. We consider here the extension of these results to higher degree systems. We restrict our attention to systems that can be characterized by a finite set of Volterra kernels, $\{h_n(\tau_1, \ldots, \tau_n): n=0, 1, 2, \ldots, N\}$, and we examine only one of the kernels at a time.

The class of kernels that can be realized by means of a finite array of linear systems and multipliers can be characterized most easily in the transform domain. We define a kernel transform pair by

$$h_n(\tau_1, \ldots, \tau_n) = \left(\frac{1}{2\pi j}\right)^n \int_{\sigma_1-j\infty}^{\sigma_1+j\infty} \cdots \int_{\sigma_n-j\infty}^{\sigma_n+j\infty} H_n(s_1, \ldots, s_n)\, e^{+s_1\tau_1+\ldots+s_n\tau_n}\, ds_1 \ldots ds_n \tag{1}$$

and

$$H_n(s_1, \ldots, s_n) = \int_{-\infty}^{+\infty} \cdots \int_{-\infty}^{+\infty} h_n(\tau_1, \ldots, \tau_n)\, e^{-s_1\tau_1 - \cdots - s_n\tau_n}\, d\tau_1 \ldots d\tau_n. \tag{2}$$

Consider first a second-degree kernel and its transform

$$h_2(\tau_1, \tau_2) \longleftrightarrow H_2(s_1, s_2).$$

The most general second-degree system that can be formed with one multiplier is shown in Fig. XVII-1. The most general second-degree system that can be formed by using N multipliers is shown in Fig. XVII-2. We find it convenient to think of the system of Fig. XVII-1 as a canonic form for second-degree systems, since all second-degree

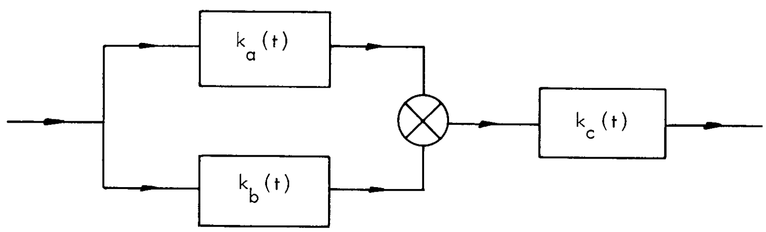

Fig. XVII-1. Canonic second-degree system.

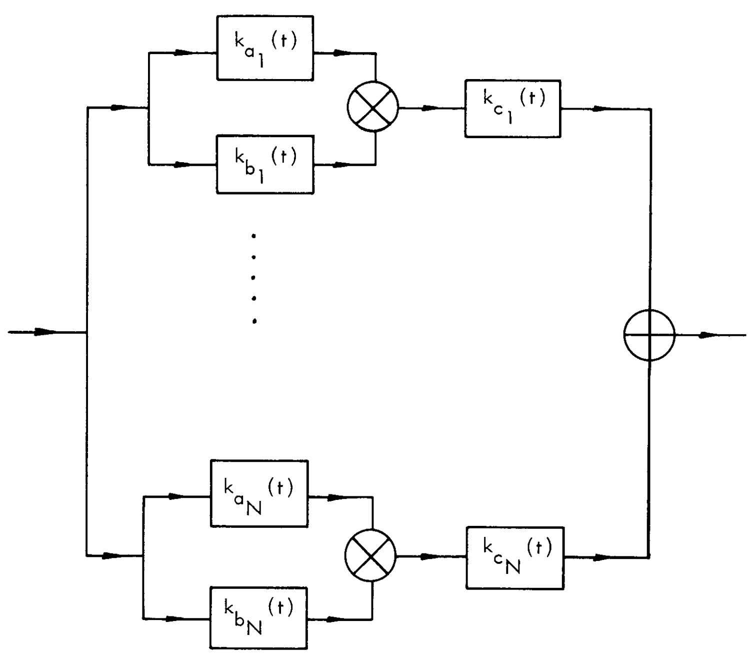

Fig. XVII-2. Second-degree system with N multipliers.

systems that can be realized exactly by means of a finite number of linear systems and multipliers can be represented as a sum of these canonic sections, as in Fig. XVII-2.

The kernel of the canonic section of Fig. XVII-1 in terms of the impulse responses $k_a(t)$, $k_b(t)$, and $k_c(t)$ of the linear systems is

$$h_2(\tau_1, \tau_2) = \int k_a(\tau_1-\sigma)\, k_b(\tau_2-\sigma)\, k_c(\sigma)\, d\sigma$$

and the corresponding kernel transform is

$$K_2(s_1, s_2) = K_a(s_1)\, K_b(s_2)\, K_c(s_1+s_2).$$

Then for the system of Fig. XVII-2, we have the kernel and kernel transform

$$g_2(\tau_1, \tau_2) = \sum_{i=1}^{N} \int k_{a_i}(\tau_1-\sigma)\, k_{b_i}(\tau_2-\sigma)\, k_{c_i}(\sigma)\, d\sigma \tag{3}$$

$$G_2(s_1, s_2) = \sum_{i=1}^{N} K_{a_i}(s_1)\, K_{b_i}(s_2)\, K_{c_i}(s_1+s_2). \tag{4}$$

If a given kernel or kernel transform can be expressed in the form (3) or (4), for some N, it can be realized with at most N multipliers; otherwise it cannot be realized exactly with a finite number of linear systems and multipliers. Examples of both types of systems have been given by Schetzen.[1]

Let us now consider higher degree systems. It is clear that the canonic third-degree system is as shown in Fig. XVII-3. It contains five linear systems and two multipliers. In Fig. XVII-4 the same system is shown with the second-degree canonic form composed

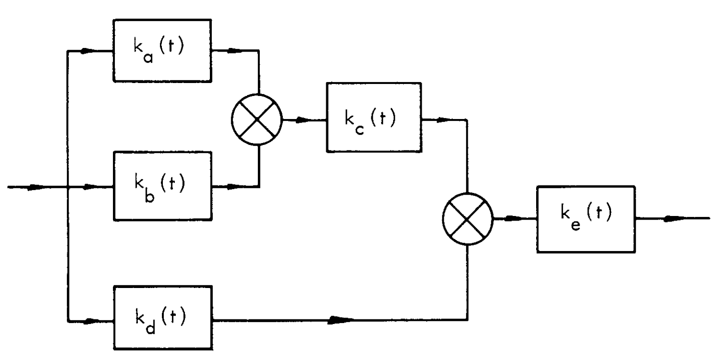

Fig. XVII-3. Canonic third-degree system.

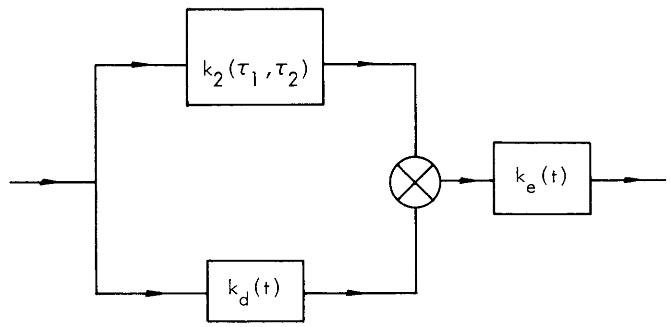

Fig. XVII-4. Alternative form for the canonic third-degree system.

of $k_a(t)$, $k_b(t)$, and $k_c(t)$ and one of the multipliers shown explicitly. The kernel and the kernel transform of this canonic section are given by

$$k_3(\tau_1, \tau_2, \tau_3) = \iint k_e(\sigma_2)\, k_d(\tau_3-\sigma_2)\, k_c(\sigma_1)\, k_a(\tau_1-\sigma_1-\sigma_2)\, k_b(\tau_2-\sigma_1-\sigma_2)\, d\sigma_1 d\sigma_2$$

$$K_3(s_1, s_2, s_3) = K_a(s_1)\, K_b(s_2)\, K_c(s_1+s_2)\, K_d(s_3)\, K_e(s_1+s_2+s_3)$$

or

$$k_3(\tau_1, \tau_2, \tau_3) = \int k_e(\sigma_2)\, k_d(\tau_3-\sigma_2)\, k_2(\tau_1-\sigma_2, \tau_2-\sigma_2)\, d\sigma_2$$

$$K_3(s_1, s_2, s_3) = K_2(s_1, s_2)\, K_d(s_3)\, K_e(s_1+s_2+s_3).$$

If a third-degree system has a kernel transform $H_3(s_1, s_2, s_3)$ that can be expressed as

$$H_3(s_1, s_2, s_3) = \sum_{i=1}^{N} K_{a_i}(s_1)\, K_{b_i}(s_2)\, K_{c_i}(s_1+s_2)\, K_{d_i}(s_3)\, K_{e_i}(s_1+s_2+s_3)$$

for some N, then it can be realized exactly with at most 2N multipliers. If it cannot be expressed in this form, then it is impossible to realize the system exactly with a finite number of linear systems and multipliers.

Now, for the fourth-degree systems, the situation is slightly more complicated. Consider the systems of Figs. XVII-5 and XVII-6. Each of them represents a fourth-degree system and is composed of seven linear systems and three multipliers, but the two forms are essentially different; that is, no block diagram manipulations can reduce one of these forms to the other. Hence, for fourth-degree systems, we have two canonic forms. It is clear that any fourth-degree system that can be realized with three or less multipliers can be arranged in one of these two canonic forms. For example, the fourth-degree system shown

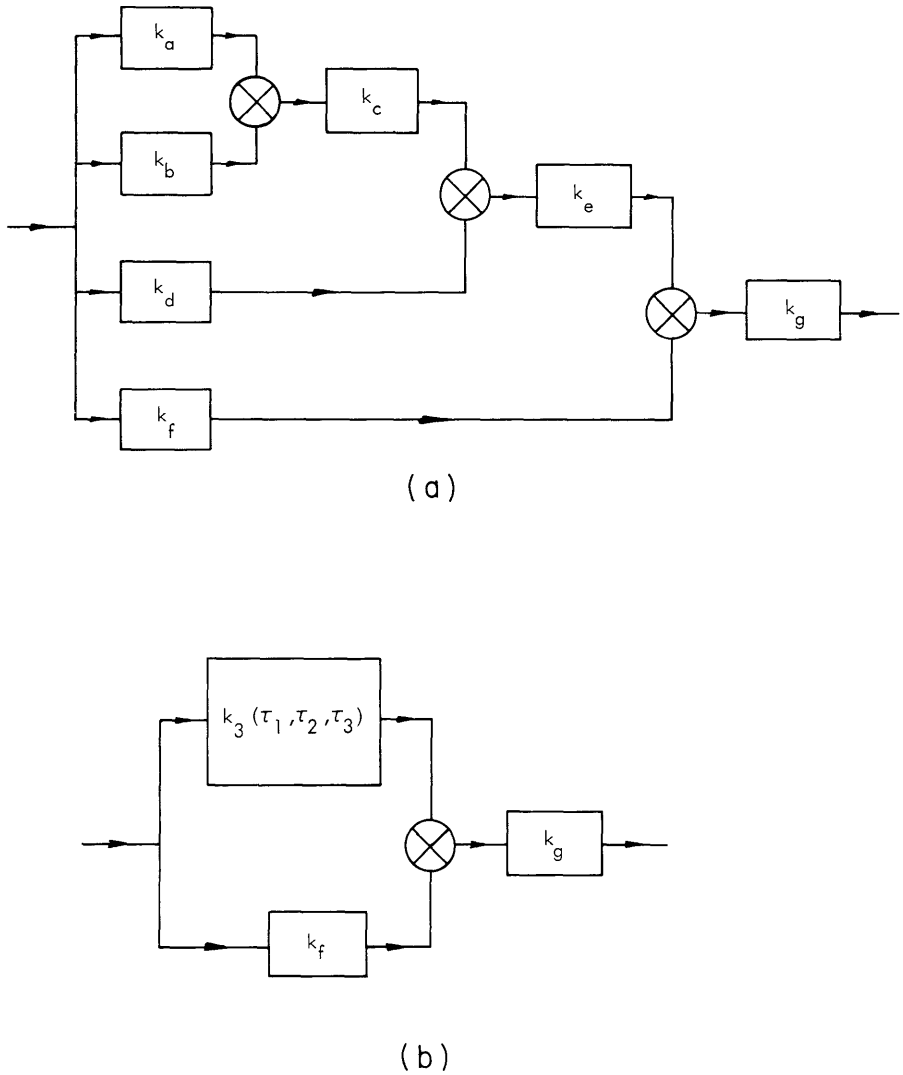

Fig. XVII-5. First canonic form for the fourth-degree systems.

in Fig. XVII-7. can be placed in the second form.

The kernel and kernel transforms for the canonic form of Fig. XVII-5 are given by

$$k_{41}(\tau_1, \tau_2, \tau_3, \tau_4) = \iiint k_g(\sigma_3)\, k_f(\tau_4-\sigma_3)\, k_e(\sigma_2)\, k_d(\tau_3-\sigma_2-\sigma_3)\, k_c(\sigma_1)\, k_b(\tau_2-\sigma_1-\sigma_2-\sigma_3)\, k_a(\tau_1-\sigma_1-\sigma_2-\sigma_3)\, d\sigma_1 d\sigma_2 d\sigma_3$$

$$K_{41}(s_1, s_2, s_3, s_4) = K_a(s_1)\, K_b(s_2)\, K_c(s_1+s_2)\, K_d(s_3)\, K_e(s_1+s_2+s_3)\, K_f(s_4)\, K_g(s_1+s_2+s_3+s_4)$$

or

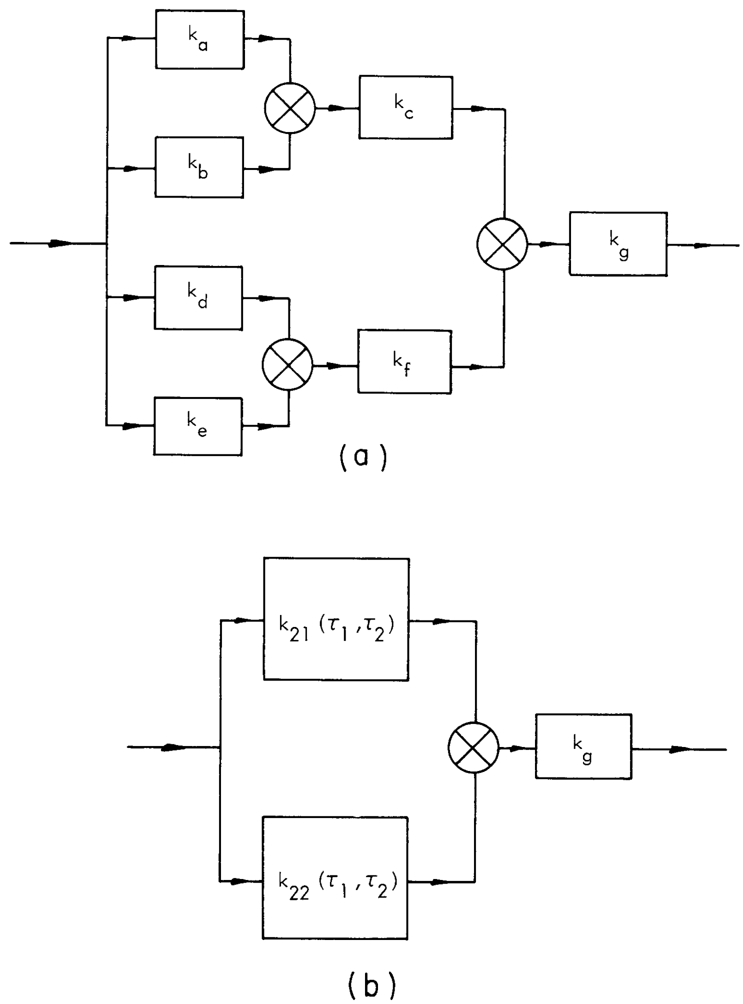

Fig. XVII-6. Second canonic form for the fourth-degree systems.

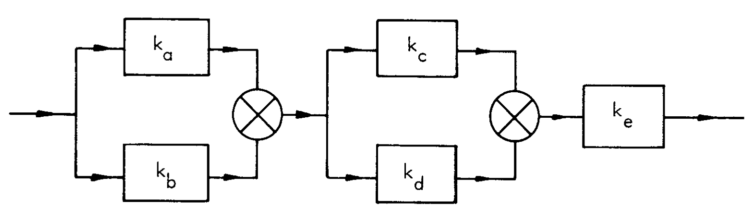

Fig. XVII-7. Fourth-degree system with two multipliers.

$$k_{41}(\tau_1, \tau_2, \tau_3, \tau_4) = \int k_g(\sigma_3)\, k_f(\tau_4-\sigma_3)\, k_3(\tau_1-\sigma_3, \tau_2-\sigma_3, \tau_3-\sigma_3)\, d\sigma_3$$

$$K_{41}(s_1, s_2, s_3, s_4) = K_3(s_1, s_2, s_3)\, K_f(s_4)\, K_g(s_1+s_2+s_3+s_4),$$

where $k_3(\tau_1, \tau_2, \tau_3)$ is the kernel of the third-degree section within the fourth-degree section.

For the canonic form of Fig. XVII-6, the kernel and kernel transform are given by

$$k_{42}(\tau_1, \tau_2, \tau_3, \tau_4) = \iiint k_g(\sigma_3)\, k_f(\sigma_2)\, k_c(\sigma_1)\, k_a(\tau_1-\sigma_1-\sigma_3)\, k_b(\tau_2-\sigma_1-\sigma_3)\, k_d(\tau_3-\sigma_2-\sigma_3)\, k_e(\tau_4-\sigma_2-\sigma_3)\, d\sigma_1 d\sigma_2 d\sigma_3$$

$$K_{42}(s_1, s_2, s_3, s_4) = K_a(s_1)\, K_b(s_2)\, K_c(s_1+s_2)\, K_d(s_3)\, K_e(s_4)\, K_f(s_3+s_4)\, K_g(s_1+s_2+s_3+s_4)$$

or

$$k_{42}(\tau_1, \tau_2, \tau_3, \tau_4) = \int k_g(\sigma_3)\, k_{21}(\tau_1-\sigma_3, \tau_2-\sigma_3)\, k_{22}(\tau_3-\sigma_3, \tau_4-\sigma_3)\, d\sigma_3$$

$$K_{42}(s_1, s_2, s_3, s_4) = K_{21}(s_1, s_2)\, K_{22}(s_3, s_4)\, K_g(s_1+s_2+s_3+s_4),$$

where $k_{21}(\tau_1, \tau_2)$ and $k_{22}(\tau_3, \tau_4)$ represent the second-degree canonic sections within the fourth-degree canonic section.

If a given fourth-degree system is characterized by a kernel transform $H_4(s_1, s_2, s_3, s_4)$, which can be expressed as

$$H_4(s_1, s_2, s_3, s_4) = \sum_{i=1}^{N_1} K_{41_i}(s_1, s_2, s_3, s_4) = + \sum_{i=1}^{N_2} K_{42_i}(s_1, s_2, s_3, s_4) \tag{5}$$

for some N_1 and N_2, then the system can be realized exactly with at most $3(N_1+N_2)$ multipliers. If the kernel transform cannot be expressed in the form of (5), then it is impossible to realize the system exactly with a finite number of multipliers.

For higher degree systems we shall have more canonic sections. A fifth-degree system may be formed as the product of a fourth-degree and a first-degree system, and the fourth-degree system may be obtained in either of the two forms given above, or we may obtain the fifth-degree system as the product of a third-degree system and a second-degree system. A sixth-degree system may be obtained as the product of a fifth-degree system and a first-degree system, a fourth-degree system and a second-degree system, or a third-degree system and a third-degree system, with all possible forms for each.

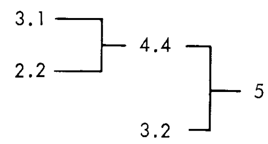

(a) TREE FOR A FIFTH-DEGREE SYSTEM

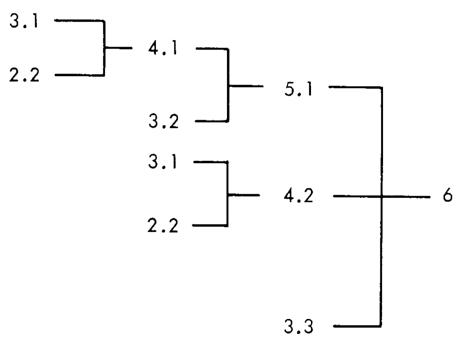

(b) TREE FOR A SIXTH-DEGREE SYSTEM

Fig. XVII-8. Trees showing canonic structures.

Although this nomenclature of canonic forms becomes rapidly complex as the degree of the system is increased, we may use the concept of a tree to summarize the process concisely, and to arrive at an expression for the number of different canonic sections for an n^{th}-degree system. The trees for the fifth-degree and the sixth-degree cases are shown in Fig. XVII-8.

We now observe that the number of different canonic sections, C(n), for an n^{th}-degree system is obtained from the expression

$$C(n) = \sum_{k=1}^{\left[\frac{n}{2}\right]} C(n-k)\, C(k), \qquad n \geq 2 \tag{6}$$

$$C(1) = 1,$$

where $[\cdot]$ denotes the greatest integer function. For example, the number of canonic sections for n = 7 is given by (6) by

$$C(7) = C(6)\, C(1) + C(5)\, C(2) + C(4)\, C(3). \tag{7}$$

From Fig. XVII-8, or repeated use of (6), we have C(6) = 6, C(5) = 3, C(4) = 2, and C(3) = C(2) = C(1) = 1, and hence, from (7), C(7) = 11. For n = 8, we have

$$C(8) = C(7)\, C(1) + C(6)\, C(2) + C(5)\, C(3) + C(4)\, C(4) = 24.$$

The tree corresponding to n = 8 is shown in Fig. XVII-9.

Thus we see that by forming the tree, and following each path in the tree, we may obtain quickly the form in which we must be able to express the kernel transform of an n^{th}-degree system in order that the system be realizable exactly by a finite number of linear systems and multipliers. For higher degree systems the expressions will not be simple, but we have exhibited a procedure for obtaining them with a minimum of effort.

Hence, given the kernel transform of an n^{th}-degree system, we may test that transform to determine whether or not it is realizable exactly with a finite number of linear systems and multipliers.

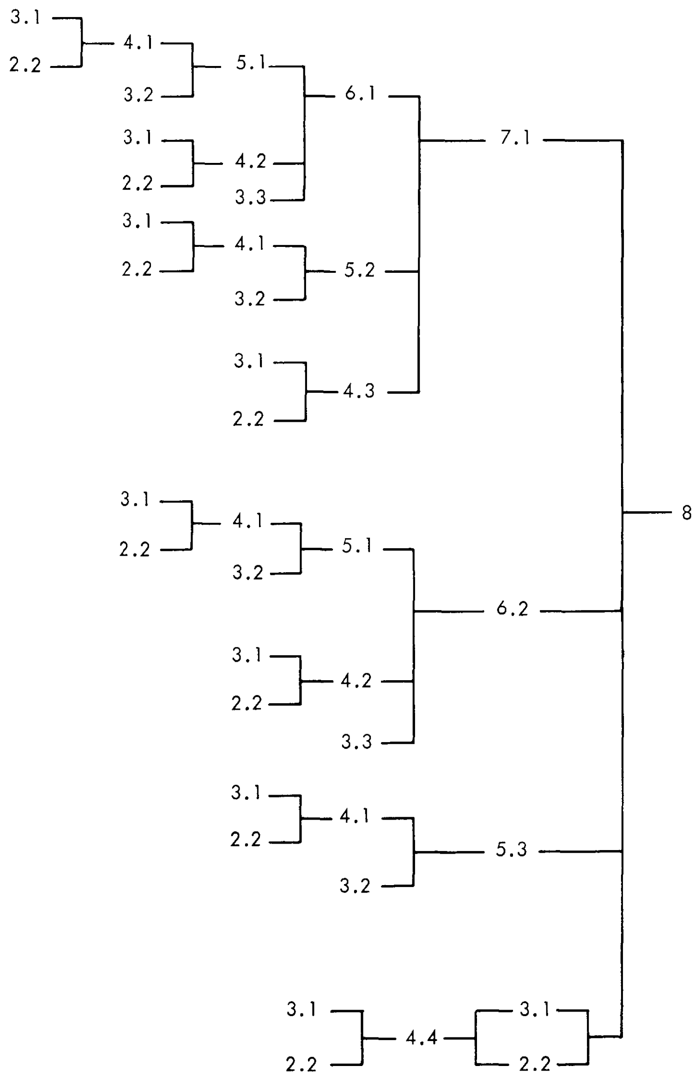

Fig. XVII-9. Tree for an eighth-degree system.

It should be noted that, in any particular case, it is not necessary to perform the test of a kernel for exact realizability in one step. One proceeds by means of a sequence of simpler tests from the higher degree side of the tree through the lower degree branches as far as possible. Following any path completely through the tree indicates that exact synthesis with linear systems and multipliers is possible; if it is impossible to follow any path completely through the tree, the synthesis is not possible. Even when the exact synthesis is not found, proceeding as far as possible through the tree reduces the synthesis problem from the synthesis of one higher degree kernel to the synthesis of several lower degree kernels, which constitutes a significant reduction.

The procedures discussed above are illustrated by two examples.

Example 1

Consider the kernel transform

$$H_4(s_1, s_2, s_3, s_4) = s_4 \Big/ (s_1s_2s_3s_4 + 2s_1s_2s_3 + s_1s_2s_4 + s_1s_3s_4 + s_2s_3s_4$$
$$+ 2s_1s_2 + 2s_1s_3 + 2s_2s_3 + s_1s_4 + s_2s_4 + s_3s_4$$
$$+ 2s_1 + 2s_2 + 2s_3 + s_4 + 2). \tag{8}$$

If this kernel is to be realized exactly with a finite number of linear systems and multipliers, we must be able to express it in the form of (5). To determine if this is possible, we first try to express (8) as

$$H_4(s_1, s_2, s_3, s_4) = F(s_1, s_2, s_3)\ G(s_4)\ H(s_1+s_2+s_3+s_4);$$

this corresponds to one of the branches in the tree for a fourth-degree system. We note that it is only necessary to consider the denominator, which we denote by $D(s_1, s_2, s_3, s_4)$. We set the variables equal to zero three at a time to obtain

$$D(0, 0, 0, s_4) = s_4 + 2 \tag{9}$$

$$D(0, 0, s_3, 0) = 2s_3 + 2 \tag{10}$$

$$D(0, s_2, 0, 0) = 2s_2 + 2 \tag{11}$$

$$D(s_1, 0, 0, 0) = 2s_1 + 2. \tag{12}$$

Since (9)-(12) have no common factor other than unity, the only possible $H(\cdot)$ is unity. Also, the only possible $G(s_4)$, from (9), is $G(s_4) = (s_4+2)$. To see if this is indeed a factor, we divide $D(s_1, s_2, s_3, s_4)$ by (s_4+2) and find

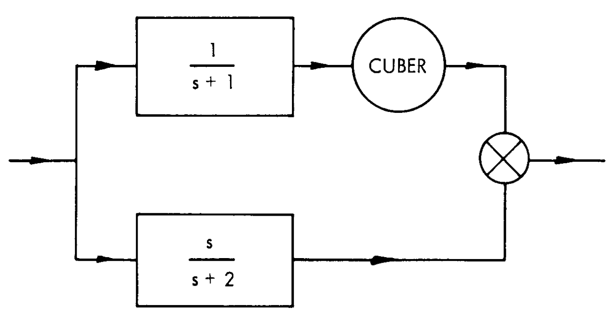

Fig. XVII-10. System with the kernel of Example 1.

$$D(s_1, s_2, s_3, s_4) = (s_4+2)(s_1s_2s_3+s_1s_2+s_1s_3+s_2s_3+s_1+s_2+s_3+1). \tag{13}$$

Now, with the help of (10)-(12), we recognize the second factor in (13) as $(s_1+1)(s_2+1)(s_3+1)$, and thus we have

$$H_4(s_1, s_2, s_3, s_4) = \left(\frac{s_4}{s_4+2}\right)\left(\frac{1}{(s_1+1)(s_2+1)(s_3+1)}\right).$$

Hence this kernel can be synthesized as shown in Fig. XVII-10.

<u>Example 2</u>

Consider the kernel transform given by

$$\begin{aligned} H_4(s_1, s_2, s_3, s_4) = (s_1+s_2)\Big/\Big(& s_1^2s_2s_3^2s_4+s_1^2s_2s_3s_4^2+s_1s_2^2s_3^2s_4+s_1s_2^2s_3s_4^2 \\ &+6s_1s_2s_3^2s_4+6s_1s_2s_3s_4^2+7s_1^2s_2s_3s_4+7s_1s_2^2s_3s_4 \\ &+2s_1^2s_2s_3^2+s_1^2s_2s_4^2+2s_1s_2^2s_3^2+s_1s_2^2s_4^2+2s_1^2s_3^2s_4 \\ &+2s_1^2s_3s_4^2+s_2^2s_3^2s_4+s_2^2s_3s_4^2+42\ s_1s_2s_3s_4 \\ &+12s_1s_2s_3^2+6s_1s_2s_4^2+10s_1^2s_2s_3+6s_1^2s_2s_4 \\ &+10s_1s_2^2s_3+6s_1s_2^2s_4+14s_1^2s_3s_4+7s_2^2s_3s_4 \\ &+8s_1s_3^2s_4+8s_1s_3s_4^2+5s_2s_3^2s_4+5s_2s_3s_4^2 \\ &+4s_1^2s_3^2+2s_1^2s_4^2+2s_2^2s_3^2+s_2^2s_4^2+60s_1s_2s_3 \\ &+36s_1s_2s_4+56s_1s_3s_4+35s_2s_3s_4+8s_1^2s_2 \\ &+8s_1s_2^2+20s_1^2s_3+12s_1^2s_4+10s_2^2s_3+6s_2^2s_4 \\ &+16s_1s_3^2+8s_1s_4^2+10s_2s_3^2+5s_2s_4^2+6s_3^2s_4 \\ &+6s_3s_4^2+48s_1s_2+80s_1s_3+48s_1s_4 \\ &+50s_2s_3+30s_2s_4+42s_3s_4+16s_1^2+8s_2^2 \\ &+12s_3^2+6s_4^2+64s_1+40s_2+60s_3+36s_4+48\Big). \end{aligned} \tag{14}$$

Again, we try to put the denominator $D(s_1, s_2, s_3, s_4)$ into a form corresponding to the $3 \cdot 1$ branch of the fourth-degree tree. We find

$$D(0,0,0,s_4) = 36s_4 + 48 = 12(3s_4+4) \tag{15}$$

$$D(0,0,s_3,0) = 12s_3^2 + 60s_3 + 48 = 12(s_3+4)(s_3+1) \tag{16}$$

$$D(0,s_2,0,0) = 8s_2^2 + 40s_2 + 48 = 8(s_2+3)(s_2+2) \tag{17}$$

$$D(s_1,0,0,0) = 16s_1^2 + 64s_1 + 48 = 16(s_1+3)(s_1+1). \tag{18}$$

Examination of (15)-(18) shows that no common factor other than 4 exists. Hence no factor of the form $H(s_1+s_2+s_3+s_4)$ can exist other than $H(\cdot) = 4$. We next attempt to find a factor that is a function of only one of the variables s_1, s_2, s_3, s_4. Division of $D(s_1, s_2, s_3, s_4)$ by each of (15)-(18) shows that such a factor cannot exist. We cannot follow the $3 \cdot 1$ branch of the tree.

We then attempt to follow the $2 \cdot 2$ branch, or to express $D(s_1, s_2, s_3, s_4)$ as

$$D(s_1,s_2,s_3,s_4) = H_2(s_1,s_2)\, K_2(s_3,s_4)$$

or as a similar expression with s_1, s_2, s_3, s_4 permuted; we have already found that no nontrivial factor of the form $H(s_1+s_2+s_3+s_4)$ can be present. Hence we write

$$D(0,0,s_3,s_4) = 6\left(s_3^2s_4 + s_3s_4^2 + 2s_3^2 + s_4^2 + 7s_3s_4 + 10s_3 + 6s_4 + 8\right). \tag{19}$$

If a factor $K_2(s_3, s_4)$ exists, it must be contained in (19). Division of $D(s_1, s_2, s_3, s_4)$ by (19) is successful, and yields a second factor; therefore we have reduced (14) to

$$H_4(s_1,s_2,s_3,s_4) = \left(\frac{s_1+s_2}{s_1^2s_2 + s_1s_2^2 + 2s_1^2 + s_2^2 + 6s_1s_2 + 8s_1 + 8s_2 + 6}\right)$$
$$\left(\frac{1}{s_3^2s_4 + s_3s_4^2 + 2s_3^2 + s_4^2 + 7s_3s_4 + 10s_3 + 6s_4 + 8}\right).$$

We have now reduced the problem to synthesis of two second-degree systems. Note that we are not yet sure whether or not either of these second-degree

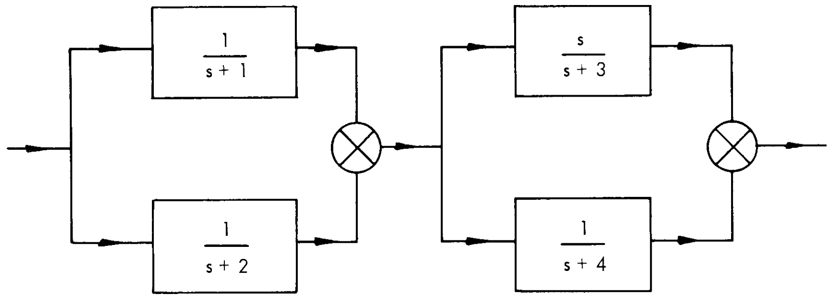

Fig. XVII-11. Realization of the kernel of Example 2.

systems is exactly realizable with a finite number of linear systems and multipliers. We may, however, examine each second-degree system separately; using the techniques given by Schetzen.[1] We find that we may realize each of them, with the system whose kernel transform is given by (14); the synthesis is shown in Fig. XVII-11.

A. M. Bush

1. M. Schetzen, Synthesis of a class of nonlinear systems, Quarterly Progress Report No. 68, Research Laboratory of Electronics, M.I.T., January 15, 1964, pp. 122-130.

B. TIME-DOMAIN SYNTHESIS TECHNIQUE FOR NONLINEAR SYSTEMS

An important feature of the convolution or superposition integral in linear system theory is the possibility of the use of impulse-train techniques.[1] The input-output relation for a linear time-invariant system may be given by the convolution integral (1), where s(t) is the system input, y(t) is the output, and $h(\tau)$ is the unit impulse response, or kernel, of the system.

$$y(t) = \int_{-\infty}^{+\infty} h(\tau)\, x(t-\tau)\, d\tau. \tag{1}$$

A generalized expression is

$$y^{(m+k)}(t) = \int_{-\infty}^{+\infty} h^{(m)}(\tau)\, x^{(k)}(t-\tau)\, d\tau, \tag{2}$$

where m and n are positive or negative integers, with $f^{(k)}(x)$ representing the k^{th} derivative of f(x) if k is positive and the k^{th} successive integration, as in (3), when k is negative.

$$f^{(-1)}(x) = \int_{-\infty}^{x} f(y)\, dy. \tag{3}$$

If some derivative of $h(\cdot)$ or $x(\cdot)$ yields only impulses, evaluation of (2) becomes very simple. This technique is useful in the evaluation of (1), in finding the transform of $h(\cdot)$, and in finding approximants to $h(\cdot)$; thus it is extremely useful in the synthesis of a linear system when $h(\cdot)$ is given.

We shall demonstrate the use of impulse-train techniques for nonlinear systems. Consider a nonlinear system for which the input-output relation (4) applies:

$$y(t) = \int_{-\infty}^{+\infty} \cdots \int_{-\infty}^{+\infty} h_n(\tau_1, \ldots, \tau_n)\, x(t-\tau_1) \ldots x(t-\tau_n)\, d\tau_1 \ldots d\tau_n, \tag{4}$$

where $x(t)$ is the input, $y(t)$ the output, and $h_n(\tau_1, \ldots, \tau_n)$ the kernel of the system. This relation may be generalized just as in the linear case:

$$y^{(m+k)}(t) = \int_{-\infty}^{+\infty} \cdots \int_{-\infty}^{+\infty} h_n^{(m)}(\tau_1, \ldots, \tau_n)\, x^{(k)}(t-\tau_1) \ldots x^{(k)}(t-\tau_n)\, d\tau_1 \ldots d\tau_n, \tag{5}$$

where the superscripts on $y(\cdot)$ and $x(\cdot)$ have the same significance as in (2), and we define

$$h_n^{(m)}(\tau_1, \ldots, \tau_n) = \frac{\partial^{nm} h_n(\tau_1, \ldots, \tau_n)}{\partial \tau_n^m \ldots \partial \tau_1^m}$$

for m positive. For $m = -1$, we define

$$h_n^{(-1)}(\tau_1, \ldots, \tau_n) = \int_{-\infty}^{\tau_n} \cdots \int_{-\infty}^{\tau_1} h_n(\eta_1, \ldots, \eta_n)\, d\eta_1 \ldots d\eta_n. \tag{6}$$

For m any negative integer, $h_n^{(m)}(\tau_1, \ldots, \tau_n)$ is found by repeated application of (6).

Although (5) is true for any n, it appears to be most useful for $n = 2$, since for this case we may often use graphical techniques. Examples of the use of (5) for the calculation of kernel transforms and the synthesis of a given kernel for second-degree systems will be given.

Example 1

Consider the second-degree kernel given by

$$h_2(\tau_1, \tau_2) = u_{-1}(\tau_1)\, u_{-1}(1-\tau_1)\, u_{-1}(\tau_2)\, u_{-1}(1-\tau_2) \tag{7}$$

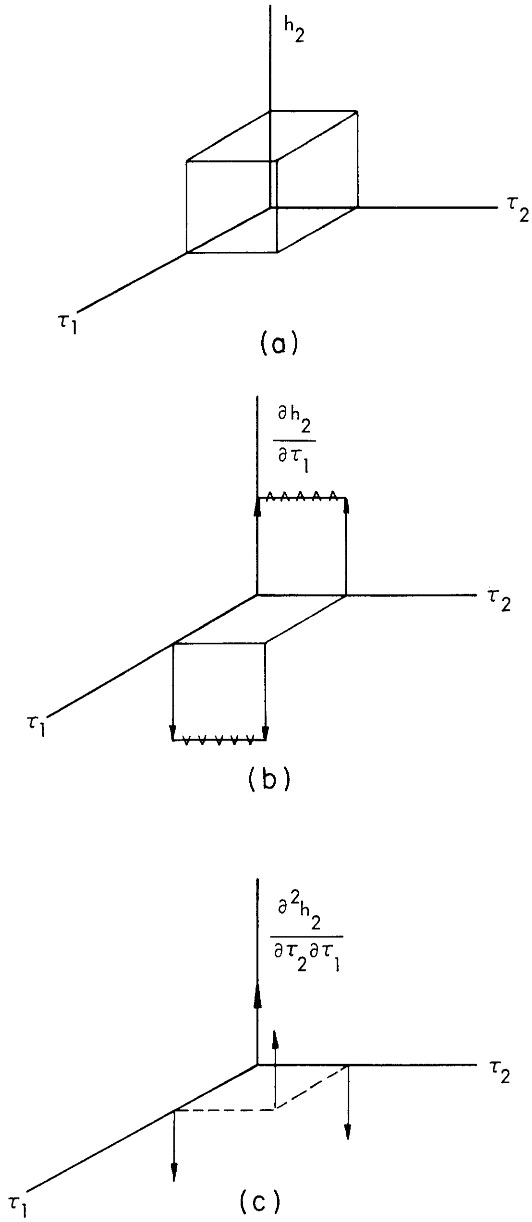

Fig. XVII-12. The kernel of Example 1.

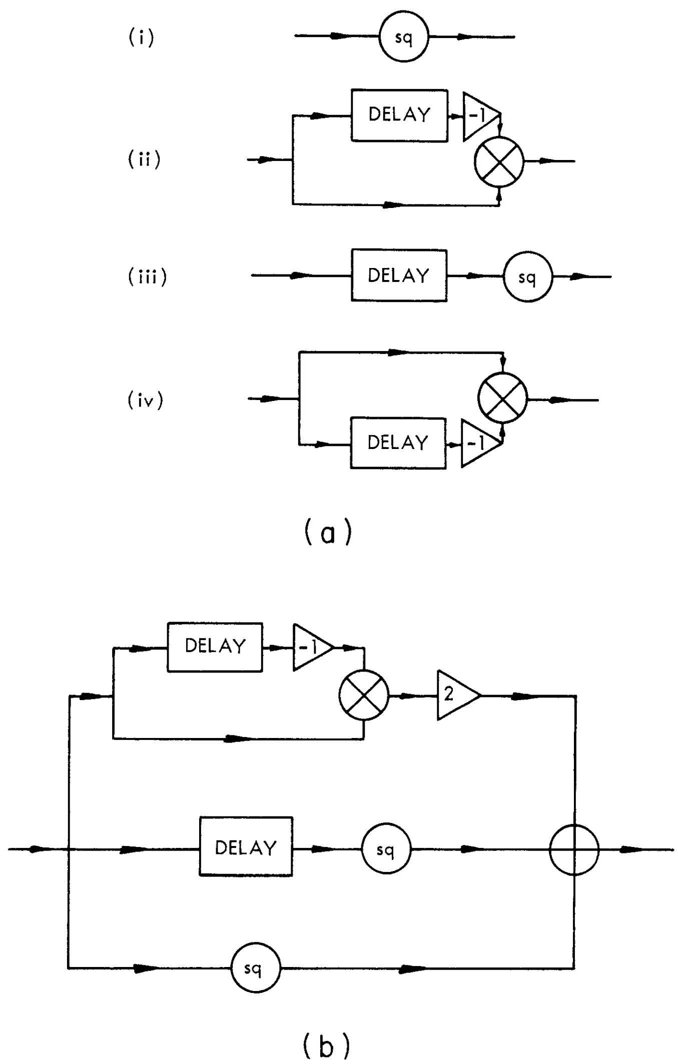

Fig. XVII-13. Realization of $\frac{\partial^2 h_2}{\partial\tau_1 \partial\tau_2}$ of Example 1.

and sketched in Fig. XVII-12a. Form the partial derivatives with respect to τ_1 and then with respect to τ_2. This may be accomplished either graphically or analytically, with the result

$$\frac{\partial h_2}{\partial \tau_1} = [u_o(\tau_1)-u_o(1-\tau_1)]\, u_{-1}(\tau_2)\, u_{-1}(1-\tau_2)$$

$$\frac{\partial h_2}{\partial \tau_2 \partial \tau_1} = u_o(\tau_1)\, u_o(\tau_2) - u_o(\tau_1)\, u_o(1-\tau_2) + u_o(1-\tau_1)\, u_o(1-\tau_2) - u_o(1-\tau_1)\, u_o(\tau_2) \tag{8}$$

These partial derivatives are sketched in Fig. XVII-12b and 12c. A type of singularity which we shall call an impulsive fence occurs in the partial with respect to τ_1 (Fig. XVII-12b).

The four impulses of the second partial can be realized as shown in Fig. XVII-13a, and combined as a sum to give the system of Fig. XVII-13b, which is a realization of the second partial derivative. Simplification yields the equivalent system shown in Fig. XVII-14. Precascading an ideal integrator, as in Fig. XVII-15, yields a system that realizes the original kernel. Note that only one integrator is required, although two differentiations were performed. Simplification yields the system of Fig. XVII-16.

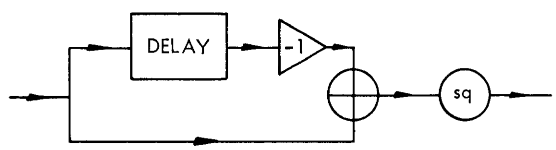

Fig. XVII-14. Simplified realization of $\frac{\partial^2 h_2}{\partial \tau_2 \partial \tau_1}$.

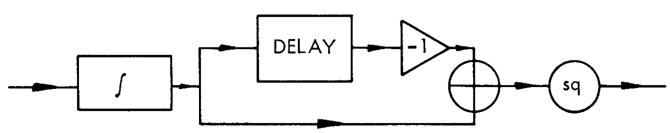

Fig. XVII-15. Realization of the kernel $h_2(\tau_1, \tau_2)$ of Example 1.

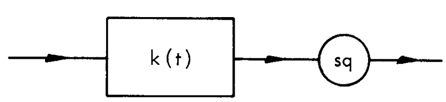

Fig. XVII-16. Simplified realization of the kernel of Example 1, with $k(t) = u_{-1}(t)\, u_{-1}(1-t)$.

Of course, in this simple example, we could have found the system of Fig. XVII-16 directly from the expression for the kernel (7).

We may also use this technique to obtain the kernel transform, as in (9) and (10), since the transforms of the components of the singular kernel of Fig. XVII-12c can be written by inspection. Factoring the transform expression of (10) to separate variables, we obtain the transform expression (11). The system of Fig. XVII-16 is recognizable from this form also.

$$\frac{\partial^2 h_2}{\partial \tau_2 \partial \tau_1} \longleftrightarrow 1 + e^{-s_1} e^{-s_2} - e^{-s_1} - e^{-s_2} \tag{9}$$

$$h_2 \longleftrightarrow \frac{1 + e^{-s_1} e^{-s_2} - e^{-s_1} - e^{-s_2}}{s_1 s_2} \tag{10}$$

$$H_2(s_1, s_2) = \left(\frac{1 - e^{-s_1}}{s_1}\right)\left(\frac{1 - e^{-s_2}}{s_2}\right). \tag{11}$$

Example 2

Consider the second-degree system characterized by

$$h_2(\tau_1, \tau_2) = (1-\tau_1-\tau_2)\, u_{-1}(1-\tau_1-\tau_2)\, u_{-1}(\tau_1)\, u_{-1}(\tau_2) \tag{12}$$

and shown in Fig. XVII-17a. Partial differentiation of this kernel yields

$$\frac{\partial h_2}{\partial \tau_1} = -u_{-1}(1-\tau_1-\tau_2)\, u_{-1}(\tau_1)\, u_{-1}(\tau_2) + (1-\tau_2)\, u_{-1}(1-\tau_2)\, u_{-1}(\tau_2)\, u_o(\tau_1)$$

$$\begin{aligned}\frac{\partial^2 h_2}{\partial \tau_2 \partial \tau_1} &= u_o(1-\tau_1-\tau_2)\, u_{-1}(\tau_1)\, u_{-1}(\tau_2) - u_{-1}(1-\tau_1)\, u_{-1}(\tau_1)\, u_o(\tau_2) \\ &\quad u_{-1}(1-\tau_2)\, u_{-1}(\tau_2)\, u_o(\tau_1) + u_o(\tau_1)\, u_o(\tau_2).\end{aligned} \tag{13}$$

These partial derivatives are sketched in Fig. XVII-17b and 17c.

Let us find the transform of the kernel (12). We shall look at the derivative (13), taking each term separately and summing. The transform of the second partial derivative is

$$1 - \frac{1 - e^{-s_1}}{s_1} - \frac{1 - e^{-s_2}}{s_2} + \frac{e^{-s_1} - e^{-s_2}}{s_2 - s_1}.$$

Simplification yields

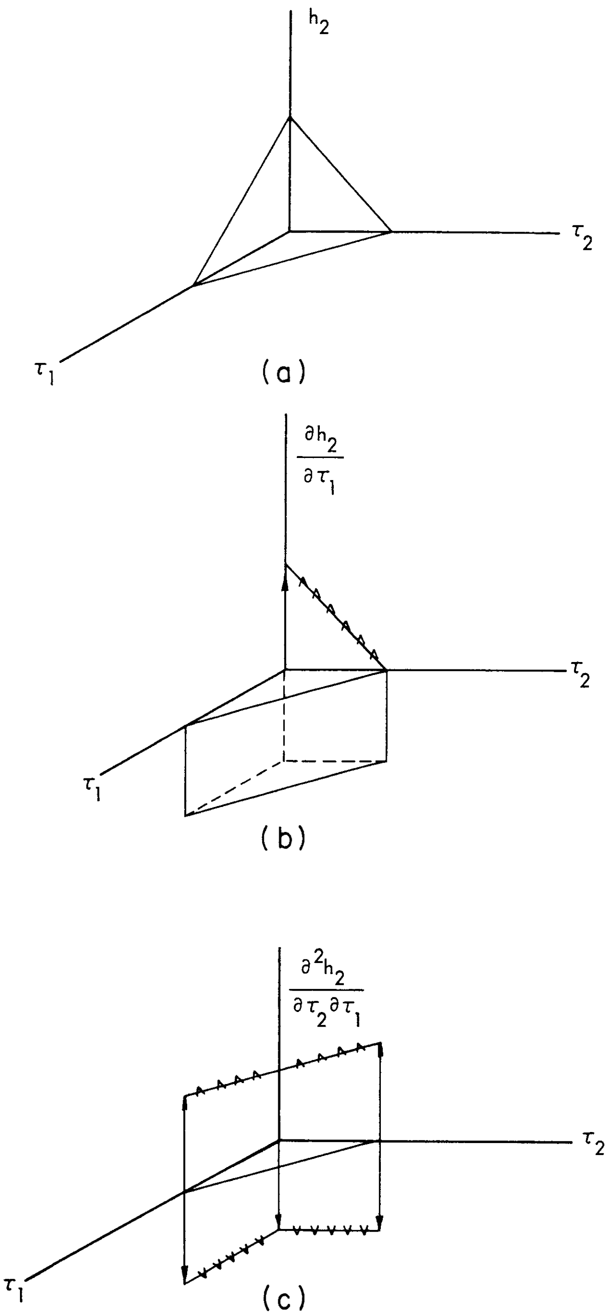

Fig. XVII-17. The kernel of Example 2.

$$\frac{s_1^2\left(1 - s_2 - e^{-s_2}\right) - s_2^2\left(1 - s_1 - e^{-s_1}\right)}{s_1 s_2 (s_2 - s_1)}$$

as the transform of the second partial derivative, and hence we have

$$H_2(s_1, s_2) = \frac{s_1^2\left(1 - s_2 - e^{-s_2}\right) - s_2^2\left(1 - s_1 - e^{-s_1}\right)}{s_1^2 s_2^2 (s_2 - s_1)}.$$

Some important observations can be made from these examples. From the kernel transforms of Example 1 and Example 2, we can see that the first kernel is of the class that can be realized exactly with a finite number of linear systems and multipliers, while the kernel of the second example cannot.

We might attempt to approximate an arbitrary kernel $h_2(\tau_1, \tau_2)$ with planes, so that we could differentiate with respect to τ_1 and τ_2 to obtain a new function consisting of impulses and impulsive fences; if we could find a system that realized this singular kernel, then the original kernel would be realized by this system cascaded after an ideal integrator. Manipulation of the resulting system as in Example 1 might lead to a quite simple realization.

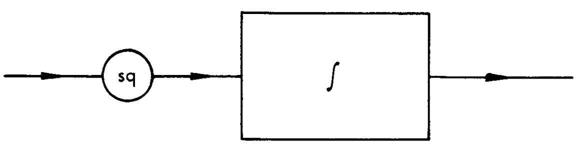

Fig. XVII-18. A system whose kernel is an impulsive function.

The second example shows, however, that not any impulsive fence is realizable with a finite number of multipliers and linear systems. In fact, a little reflection shows that the only impulsive fences that can be realized with one multiplier and linear systems are those lying along lines intersecting the τ_1 or τ_2 axes at a 45° angle, or along lines parallel to the axes. Such an impulsive fence is

$$f(\tau_1, \tau_2) = u_o(\tau_1 - \tau_2)\, u_{-1}(\tau_1)\, u_{-1}(\tau_2)$$

which has the transform

$$F(s_1, s_2) = \frac{1}{s_1 + s_2}.$$

This is realizable as shown in Fig. XVII-18.

A unit impulsive fence passing through the origin of the τ_1, τ_2 plane at any other angle will not be realizable with a finite number of linear systems and multipliers. For example,

$$g(\tau_1, \tau_2) = u_o(\tau_1 - a\tau_2)\, u_{-1}(\tau_1)\, u_{-1}(\tau_2)$$

has the transform

$$G(s_1, s_2) = \frac{1}{s_2 + as_1}.$$

Thus if we wish to approximate a kernel with planes, in an effort to find a realization for the system from a finite number of linear systems and multipliers, then we must choose the approximating planes so that differentiation with respect to τ_1 and τ_2 yields a sum of impulses and impulsive fences, with the impulsive fences occurring only along the 45° lines or parallel to the axes. Convenient methods for finding such approximants are under investigation.

A. M. Bush

References

1. E. A. Guillemin, Theory of Linear Physical Systems (John Wiley and Sons, Inc., New York, 1963), p. 386.

C. MODEL FOR MAGNETIC TAPE NOISE

1. Introduction

Magnetic tape noise is frequently represented as the output of a linear filter excited by a train of positive and negative impulses having random areas and random interarrival times. The probability that any impulse is positive or negative is a function of the magnetic state of the tape. For the erased state, the probability of being either positive or negative is one-half. For positive saturation, the probability is one for a positive impulse, and zero for a negative impulse.

This model is intuitively reasonable, since the magnetic coating of a recording tape is composed of small, acicular, ferrite particles (magnetic dipoles) fixed in a plastic binder. The direction of the individual magnetic dipole moments determine whether the corresponding voltage pulse produced by the reproducing head is positive or negative. And the direction of the individual dipoles is a function of the magnetic state of the tape which is determined by the external magnetizing field and the interaction of the particles.

The autocorrelation function and power density spectrum of a train of impulses with random areas and random interarrival times[1] are given by

$$R(\tau) = \overline{N}\left[\overline{m^2}\, u_o(\tau) + \sum_{j=1}^{\infty} \overline{m_k m_{k+j}} \left(P_{\eta_j}(\tau) + P_{\eta_j}(-\tau)\right)\right] \tag{1}$$

$$S(\omega) = \overline{N}\left[\overline{m^2} + 2\mathrm{Re} \sum_{j=1}^{\infty} \overline{m_k m_{k+j}}\, M_{\eta_j}(\omega)\right]. \tag{2}$$

The average number of impulses per second is $\overline{N}$, m_k is the area of the k^{th} impulse, $\overline{m^2} = E[m^2]$ and $\overline{m_k m_{k+j}} = E[m_k m_{k+j}]$, $P_{\eta_j}(\tau)$ is the probability that the waiting time, η, to the j^{th} impulse is τ, and $M_{\eta_j}(\omega)$ is the characteristic function of $P_{\eta_j}(\tau)$.

In this report we wish to show the change in the power density spectrum with variations in the average value of the impulse train. We shall do this for two conditions; first, with the signs of the impulses statistically independent; second, when they are nonindependent and the dependence can be represented by a first-order Markov process.

Rewriting (1) and (2) as functions of the signs of the impulses gives

$$R(\tau) = \overline{N}\left[\overline{m^2}\, u_o(\tau) + \left|\overline{m}\right|^2 \sum_{j=1}^{\infty} \overline{s_k s_{k+j}} \left(P_{\eta_j}(\tau) + P_{\eta_j}(-\tau)\right)\right] \tag{3}$$

$$S(\omega) = \overline{N}\left[\overline{m^2} + 2\left|\overline{m}\right|^2 \operatorname{Re} \sum_{j=1}^{\infty} \overline{s_k s_{k+j}}\, M_{\eta_j}(\omega)\right], \tag{4}$$

where s_k is the sign of the k^{th} impulse, and $\overline{s_k s_{k+j}} = E[s_k s_{k+j}]$. We have also assumed that the magnitudes of the k^{th} and $k+j^{th}$ impulses are statistically independent.

The waiting-time probabilities between adjacent impulses are assumed to be independent and exponential, this corresponds to a Poisson distribution.

2. Case I: Impulse Signs Statistically Independent

When the signs of the k^{th} and $k+j^{th}$ impulses are statistically independent,

$$\overline{s_k s_{k+j}} = E[s_k s_{k+j}] = E[s_k]\, E[s_{k+j}]. \tag{5}$$

Assuming a stationary impulse train gives

$$\overline{s_k s_{k+j}} = E^2[s] \tag{6}$$

and

$$E[s] = P(s=+1) - P(s=-1). \tag{7}$$

Thus the autocorrelation function is

$$R(\tau) = \begin{cases} \overline{N}\left[\overline{m^2}\, u_o(\tau) + \left|\overline{m}\right|^2 (P_+ - P_-)^2 \displaystyle\sum_{j=1}^{\infty} \overline{N} \frac{(\overline{N}\tau)^{j-1}}{(j-1)!} e^{-\overline{N}\tau}\right] & \tau \geq 0 \\ \overline{N}\left|\overline{m}\right|^2 (P_+ - P_-)^2 \displaystyle\sum_{j=1}^{\infty} \overline{N} \frac{(-\overline{N}\tau)^{j-1}}{(j-1)!} e^{\overline{N}\tau} & \tau < 0 \end{cases} \tag{8}$$

which reduces to

$$R(\tau) = \overline{N}\left[\overline{m^2}u_o(\tau) + \overline{N}|\overline{m}|^2(P_+ - P_-)^2\right]. \tag{9}$$

The power density spectrum is

$$S(\omega) = \overline{N}\left[\overline{m^2} + \overline{N}|\overline{m}|^2(P_+ - P_-)^2\ u_o(\omega)\right], \tag{10}$$

where $P_+ = P(s=+1)$, and $P_- = P(s=-1)$.

The effect on this power density spectrum as the average value of the impulse train changes is limited to a variation in the area of the impulse at the origin. As shown in

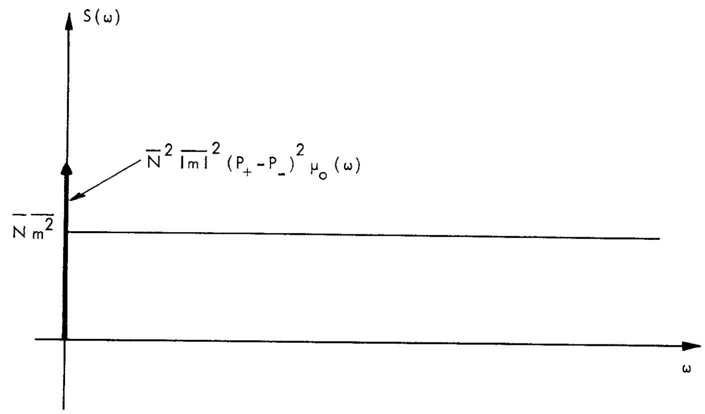

Fig. XVII-19. Power density spectrum of a series of independent impulses.

Fig. XVII-19, the impulse is zero for zero average value $\left(P_+ = P_- = \frac{1}{2}\right)$ and has its maximum value when $(P_+ = 1,\ P_- = 0)$ or $(P_+ = 0,\ P_- = 1)$.

3. Case 2: Impulse Signs Nonindependent

a. Unspecified Dependence

When the sign of the k^{th} and $k+j^{th}$ impulses are not statistically independent, the expectation of their product can be written in the following general form.

$$\begin{aligned}\overline{s_k s_{k+j}} &= P(s_k = +1, s_{k+j} = +1) + P(s_k = -1, s_{k+j} = -1) \\ &\quad -P(s_k = +1, s_{k+j} = -1) - P(s_k = -1, s_{k+j} = +1)\end{aligned} \tag{11}$$

$$\begin{aligned}&= P(s_k = +1)[P(s_{k+j} = +1 \mid s_k = +1) - P(s_{k+j} = -1 \mid s_k = +1)] \\ &\quad +P(s_k = -1)[P(s_{k+j} = -1 \mid s_k = -1) - P(s_{k+j} = 1 \mid s_k = -1)].\end{aligned} \tag{12}$$

This can be written more compactly

$$\overline{s_k s_{k+j}} = P_+\left(P_{++}^{(j)} - P_{+-}^{(j)}\right) + P_-\left(P_{--}^{(j)} - P_{-+}^{(j)}\right), \tag{13}$$

where, for example, $P_{+-}^{(j)}$ is the conditional probability that the j^{th} impulse after a given positive impulse will be negative. These conditional probabilities must be determined before the power density spectrum for the dependent case can be evaluated.

b. Markov Dependence

The unconditional probabilities in Eq. 13 could be evaluated if the relation between the signs of the impulses were known (or if the interaction between the magnetic dipoles were known in the magnetic tape noise problem). Since this relation is not known, we assume initially that the sign of the k^{th} impulse is only affected by the sign of the adjacent impulse. Then the impulse sign dependence can be modeled by a first-order Markov process.

The Markov transition matrix giving the four conditional probabilities between adjacent impulses is

$$P^{(1)} = \begin{bmatrix} P_{++} & P_{+-} \\ P_{-+} & P_{--} \end{bmatrix} = \begin{bmatrix} 1 - P_{+-} & P_{+-} \\ P_{-+} & 1 - P_{-+} \end{bmatrix} \tag{14}$$

The conditional probabilities for impulses separated by j−1 impulses are given by the j^{th} transition matrix

$$\underline{P}^{(j)} = \frac{1}{P_{+-} + P_{-+}} \begin{bmatrix} P_{-+} & P_{+-} \\ P_{-+} & P_{+-} \end{bmatrix} + \frac{(1 - P_{+-} - P_{-+})^j}{P_{+-} + P_{-+}} \begin{bmatrix} P_{+-} & -P_{+-} \\ -P_{-+} & P_{-+} \end{bmatrix} \tag{15}$$

Substituting these conditional probabilities in Eq. 13 gives

$$\overline{s_k s_{k+j}} = (P_+ - P_-) \frac{(P_{-+} - P_{+-})}{(P_{-+} + P_{+-})} + 2 \frac{(P_+P_{+-} + P_-P_{-+})}{P_{+-} + P_{-+}} (1 - P_{+-} - P_{-+})^j. \tag{16}$$

Since the impulse train is stationary,

$$P_+ = \frac{P_{-+}}{P_{+-} + P_{-+}} \qquad P_- = \frac{P_{+-}}{P_{+-} + P_{-+}}$$

and Eq. 16 can then be simplified to

$$\overline{s_k s_{k+j}} = (P_+ - P_-)^2 + 4\,\frac{P_{+-}P_{-+}}{(P_{+-}+P_{-+})^2}\,(1-P_{+-}-P_{-+})^j. \tag{17}$$

The autocorrelation function is thus

$$R(\tau) = \overline{N}\left[\overline{m^2}\,u_o(\tau) + \overline{N}\,\overline{|m|}^2\,(P_+ - P_-)^2 + 4\,\overline{N}\,\overline{|m|}^2\,\frac{P_{+-}P_{-+}}{(P_{+-}+P_{-+})^2}\,(1-P_{+-}-P_{-+})\,e^{-\overline{N}|\tau|(P_{+-}+P_{-+})}\right], \tag{18}$$

and the power density spectrum is

$$S(\omega) = \overline{N}\left[\overline{m^2} + \overline{N}\,\overline{|m|}^2\,(P_+ - P_-)^2\,u_o(\omega) + 8\,\overline{|m|}^2\,\frac{P_{+-}P_{-+}}{(P_{+-}+P_{-+})^3}\,(1-P_{+-}-P_{-+})\,\frac{1}{1+\left[\dfrac{\omega}{\overline{N}(P_{+-}+P_{-+})}\right]^2}\right]. \tag{19}$$

This power density spectrum is plotted in Fig. XVII-20 for the case in which the average value is zero and for various values of P_{+-} and P_{-+} consistent with this

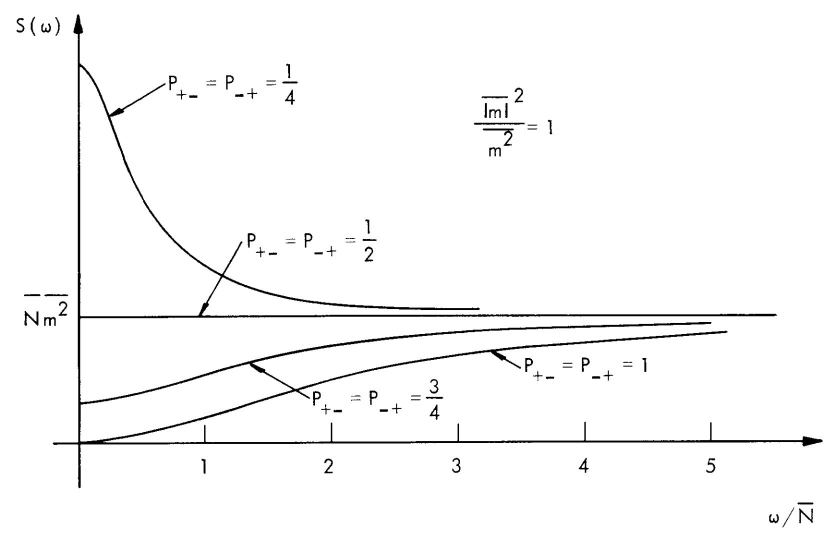

Fig. XVII-20. Power density spectrum of a series of dependent impulses.

average value. The correlation between the impulses changes the shape of the power density spectrum appreciably. As can be seen, when $P_{+-} = P_{-+} = 1$, the low-frequency power in the impulse train is small, since the impulses are alternating in sign. As

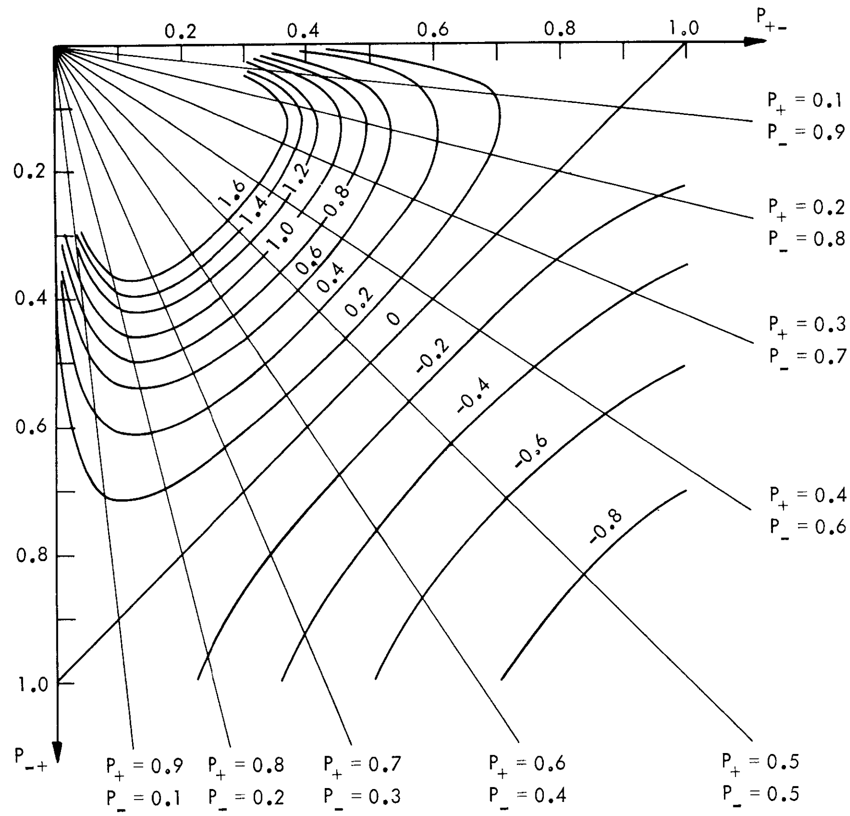

Fig. XVII-21. Contour plot of M.

P_{+-} and P_{-+} decrease, the low-frequency power increases and the half-power point shifts to lower frequencies, since the probability of longer strings of impulses with the same sign is increasing.

A fuller picture of the manner in which $S(\omega)$ varies with P_{+-}, P_{-+} and the average value is given in Fig. XVII-21. This is a contour plot of M as a function of P_{+-} and P_{-+}, where

$$M = 8 \frac{P_{+-}P_{-+}}{(P_{+-}+P_{-+})^3}(1-P_{+-}-P_{-+}) \tag{20}$$

and M is related to $S(\omega)$ by

$$S(0) - \overline{N}^2\ \overline{|m|}^2\ (P_+-P_-)^2 = \overline{N}\ \overline{m^2}\left[1+\frac{\overline{|m|}^2}{\overline{m^2}}M\right]. \tag{21}$$

Overlaid on this plot are lines relating P_{+-} and P_{-+} to the average value of the impulse train. The straight line from $P_{+-}=1$ to $P_{-+}=1$ corresponds to the statistically independent case.

4. Application to the Problem of Magnetic Tape Noise

A train of impulses with a variable average value is often used to model the source of magnetic tape noise. If the power density spectrum of this impulse train is known, then the power density spectrum of the noise at the reproducing head output is given by

$$S_o(\omega) = |F(\omega)|^2 S(\omega),$$

where $F(\omega)$ is the frequency response of the reproduction head.

A characteristic of $F(\omega)$ is that $F(0) = 0$. (An obvious consequence of the fact that the output voltage is related to the time derivative of the flux passing through the reproduction head.)

In previous papers[2,3] in which the impulse train model was used, it has been assumed that the impulses are Poisson-distributed and statistically independent. The power density spectrum of such an impulse train is given in Eq. 10. From this equation and the fact that $F(0) = 0$, we can say that the output-noise power density spectrum does not change with the average magnetization. Experimentally, we know that the noise increases with magnetization. This proves that the impulse-train model with the assumptions above is invalid.

From Eq. 19 we see that it would be possible to account for the increase in noise with magnetization with the impulse-train model and a Poisson distribution of impulses if there were correlation between the impulses. (This also makes good sense physically, since the magnetic particles interact.) In order to satisfactorily prove that correlation is the cause of the noise, however, the Markov model must be justified and the changes in P_{+-} and P_{-+} as the magnetization varies must be determined.

R. F. Bauer

References

1. D. E. Nelsen, Calculation of power density spectra for a class of randomly jittered waveforms, Quarterly Progress Report No. 74, Research Laboratory of Electronics, M.I.T., July 15, 1964, pp. 168-179.

2. D. E. Wooldridge, Signal and noise levels in magnetic tape recording, Electrical Engineering, Vol. 65, pp. 343-352, June 1946.

3. P. A. Mann, The noise of a magnetic recording tape, Arch. Elek. Übertrag. 11, 97-100 (1957).

D. CORRELATION FUNCTIONS OF QUANTIZED GAUSSIAN SIGNALS

Considerable attention has recently been given to the problem of determining the parameters that define optimum quantizers.[1,2] Many times in addition to determining the optimum quantizer parameters, it is desirable to determine the autocorrelation

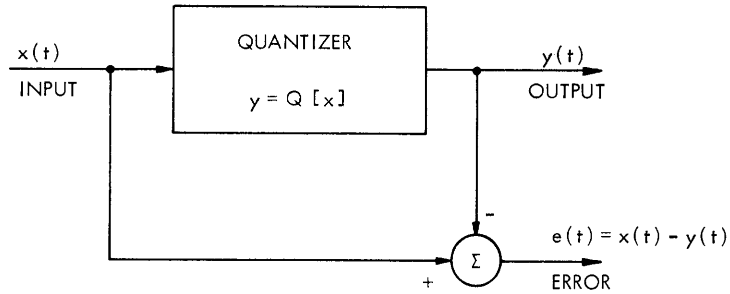

Fig. XVII-22. Diagram indicating notation.

function of the quantizer-output signal and the quantizer-error signal (see Fig. XVII-22) in terms of the autocorrelation function of the quantizer-input signal and the parameters specifying the quantizer. In this report we shall develop expressions for the output and error autocorrelation functions when the quantizer-input signal is a stationary, bivariate normal process.

We begin by considering the autocorrelation function of the quantizer-output signal y(t). By definition, this autocorrelation function[3] is

$$\phi_{yy}(\tau) = \lim_{T\to\infty} \frac{1}{2T} \int_{-T}^{T} y(t)\, y(t+\tau)\, dt. \tag{1}$$

As y(t) is a stationary process, we are able to write (1) on an ensemble basis[4] as

$$\phi_{yy}(\tau) = \int_{-\infty}^{\infty} d\eta_1 \int_{-\infty}^{\infty} d\eta_2 \left[\eta_1\eta_2 p_y(\eta_1, \eta_2; \tau)\right], \tag{2}$$

where η_1 and η_2 correspond to observation of the signal y(t) at times t and $(t+\tau)$, respectively.

Referring to the quantizer block diagram of Fig. XVII-22, we see that

$$y(t) = Q[x(t)], \tag{3}$$

where Q is a single-valued function of its argument (see Fig. XVII-23). Thus, with reference to Eqs. 2 and 3, we have for the output autocorrelation function

$$\phi_{yy}(\tau) = \int_{-\infty}^{\infty} d\xi_1 \int_{-\infty}^{\infty} d\xi_2 \left\{Q[\xi_1]Q[\xi_2]p_x(\xi_1, \xi_2; \tau)\right\}. \tag{4}$$

As we have indicated, the quantizer-input signal x(t) is assumed to be a bivariate normal process. Such a process has the amplitude probability density[5,6]

$$p_x(\xi_1, \xi_2; \tau) = \frac{1}{2\pi\left[\phi_{xx}^2(0)-\phi_{xx}^2(\tau)\right]^{1/2}} \times \exp\left\{\frac{\phi_{xx}(0)\left[(\xi_1-\nu)^2+(\xi_2-\nu)^2-2\xi_1\xi_2\phi_{xx}(\tau)\right]}{2\left[\phi_{xx}^2(0)-\phi_{xx}^2(\tau)\right]}\right\}, \tag{5}$$

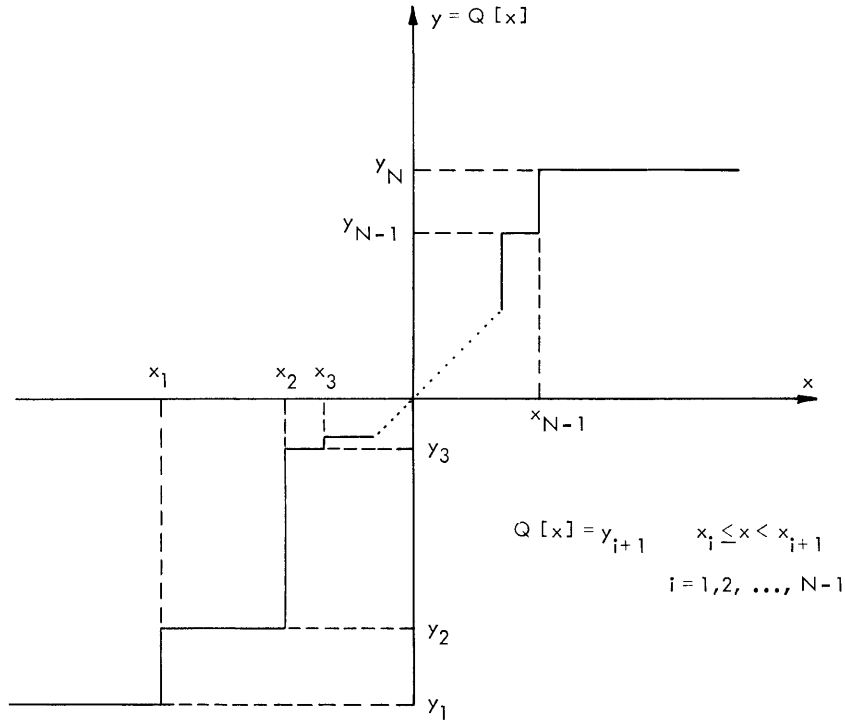

Fig. XVII-23. Quantizer transfer characteristic. The x_i are called the transition values, and the y_i representation values.

where ν is the mean value of x(t). For purposes of this report we restrict ourselves to input signals satisfying the two constraints

$$\left.\begin{aligned} \nu &= 0 \\ \phi_{xx}(0) &= 1 \end{aligned}\right\}. \tag{6}$$

These restrictions will not, as a rule, reduce the generality of the results that we shall obtain.

Combining Eqs. 4, 5, and 6, we have

$$\phi_{yy}(\tau) = \int_{-\infty}^{\infty} d\xi_1 \int_{-\infty}^{\infty} d\xi_2 \left\{ Q[\xi_1]\, Q[\xi_2] \right.$$
$$\left. \times \frac{1}{2\pi\left[1-\phi_{xx}^2(\tau)\right]^{1/2}} \exp\left[-\frac{\xi_1^2+\xi_2^2-2\xi_1\xi_2\phi_{xx}(\tau)}{2\left[1-\phi_{xx}^2(\pi)\right]}\right]\right\}. \tag{7}$$

From Fig. XVII-23 we see that the quantizer characteristic Q[x] is specified by the (N-1) equations

$$Q[x] = y_{i+1} \qquad x_i \leq x < x_{i+1} \qquad i = 1, 2, \ldots, N-1. \tag{8}$$

Here, x_o equals X_ℓ the greatest lower bound to the quantizer-input signal and x_N equals X_u, the least upper bound to the input signal. Substituting Eq. 8 in Eq. 7, we have

$$\phi_{yy}(\tau) = \frac{1}{2\pi\left[1-\phi_{xx}^2(\tau)\right]^{1/2}} \sum_{i=0}^{N-1} \sum_{k=0}^{N-1} \int_{x_i}^{x_{i+1}} d\xi_1 \int_{x_k}^{x_{k+1}} d\xi_2 \times \left\{ y_{i+1}\, y_{k+1} \exp\left[-\frac{\xi_1^2+\xi_2^2-2\xi_1\xi_2\phi_{xx}(\tau)}{2\left[1-\phi_{xx}^2(\tau)\right]}\right]\right\}. \tag{9}$$

While Eq. 9 is an acceptable form for $\phi_{yy}(\tau)$, we can obtain a different form of this equation which will yield considerably more insight into the composition of $\phi_{yy}(\tau)$ by expanding the exponential in an infinite series. In order to do this, we first multiply the exponential term by

$$\exp\left[\frac{\xi_1^2+\xi_2^2}{2}\right] \exp\left[-\frac{\xi_1^2+\xi_2^2}{2}\right].$$

Upon multiplication and collection of terms, the exponential term becomes

$$\exp\left[\frac{2\xi_1\xi_2\phi_{xx}(\tau) - \left(\xi_1^2+\xi_2^2\right)\phi_{xx}^2(\tau)}{2\left[1-\phi_{xx}^2(\tau)\right]}\right] \exp\left[-\frac{\xi_1^2+\xi_2^2}{2}\right]. \tag{10}$$

The first of these two terms can be written in the form of an infinite series through the use of Mehler's formula[7]:

$$\left[1-\phi_{xx}^2(\tau)\right]^{1/2} \sum_{m=0}^{\infty} \frac{1}{m!} H_m(\xi_1)\, H_m(\xi_2)\, \phi_{xx}^m(\tau) = \exp\left[\frac{2\xi_1\xi_2\phi_{xx}(\tau) - \left(\xi_1^2+\xi_2^2\right)\phi_{xx}^2(\tau)}{2\left[1-\phi_{xx}^2(\tau)\right]}\right]. \tag{11}$$

The Hermite polynomials $H_m(x)$ are defined by

$$\frac{d^m}{dx^m} e^{-x^2/2} = (-1)^m H_m(x)\, e^{-x^2/2}. \tag{12}$$

Making appropriate substitutions of Eqs. 10 and 11 in (9), we obtain

$$\phi_{yy}(\tau) = \frac{1}{2\pi} \sum_{i=0}^{N-1} \sum_{k=0}^{N-1} \int_{x_i}^{x_{i+1}} d\xi_1 \int_{x_k}^{x_{k+1}} d\xi_2$$

$$\times \left\{ y_{i+1}\, y_{k+1} \left[\sum_{m=0}^{\infty} \frac{1}{m!} H_m(\xi_1)\, H_m(\xi_2)\, \phi_{xx}^m(\tau) \right] \times \exp\left[- \frac{\xi_1^2 + \xi_2^2}{2} \right] \right\}. \tag{13}$$

After rearranging the terms, (13) becomes

$$\phi_{yy}(\tau) = \sum_{m=0}^{\infty} \phi_{xx}^m(\tau) \times \left\{ \frac{1}{(2\pi m!)^{1/2}} \sum_{i=0}^{N-1} y_{i+1} \int_{x_i}^{x_{i+1}} d\xi_1\, e^{-\xi_1^2/2}\, H_m(\xi_1) \right\}$$

$$\times \left\{ \frac{1}{(2\pi m!)^{1/2}} \sum_{k=0}^{N-1} y_{k+1} \int_{x_k}^{x_{k+1}} d\xi_2\, e^{-\xi_2^2/2}\, H_m(\xi_2) \right\} \tag{14}$$

or

$$\phi_{yy}(\tau) = \sum_{m=0}^{\infty} a_m^2 \phi_{xx}^m(\tau), \tag{15}$$

where

$$a_m = \frac{1}{(2\pi m!)^{1/2}} \sum_{i=0}^{N-1} y_{i+1} \int_{x_i}^{x_{i+1}} d\xi\, e^{-\xi^2/2}\, H_m(\xi), \tag{16}$$

since the two terms enclosed by braces in Eq. 10 are identical.

By using the Wiener theorem,[8] we find that the power density spectrum of the quantizer-output signal is

$$\Phi_{yy}(\omega) = \sum_{m=0}^{\infty} a_m^2 \Phi_{xx}^{*m}(\omega), \tag{17}$$

where $\Phi_{xx}(\omega)$ is the power density spectrum of the quantizer input signal. $\Phi_{xx}^{*m}(\omega)$ indicates the m^{th} convolution of $\Phi_{xx}(\omega)$ with itself. Φ_{xx}^{*o}, the term for m=0, is

$$\Phi_{xx}^{*o}(\omega) = u_o(\omega), \tag{18}$$

where $u_o(\omega)$ is the unit impulse function. We now turn our attention to the quantizer-error signal,

$$e(t) = x(t) - y(t). \tag{19}$$

From Eq. 19 we see that the autocorrelation function of the error is[9]

$$\phi_{ee}(\tau) = \phi_{xx}(\tau) + \phi_{yy}(\tau) - \phi_{xy}(\tau) - \phi_{yx}(\tau)$$

or

$$\phi_{ee}(\tau) = \phi_{xx}(\tau) + \phi_{yy}(\tau) - \phi_{xy}(\tau) - \phi_{xy}(-\tau), \tag{20}$$

since $\phi_{yx}(\tau) = \phi_{xy}(-\tau)$.

In order to evaluate (2), we must first evaluate $\phi_{xy}(\tau)$. Bussgang[10] has shown that

$$\phi_{xy}(\tau) = \beta\phi_{xx}(\tau), \tag{21}$$

where

$$\beta = \frac{1}{\sqrt{2\pi}}\int_{-\infty}^{\infty} d\xi \left\{\xi Q[\xi]\, e^{-\xi^2/2}\right\} \tag{22}$$

if x(t) is a sample function of a bivariate normal process, and Q is a single-valued function of its argument. This being the case in our problem, we proceed by evaluating β for this particular device. Substitution of the device characteristic yields

$$\beta = \frac{1}{\sqrt{2\pi}} \sum_{i=0}^{N-1} y_{i+1} \int_{x_i}^{x_{i+1}} \xi\, e^{-\xi^2/2}\, d\xi. \tag{23}$$

Comparing (23) with (16) for the case in which m=1 and realizing that $H_1(\xi) = \xi$, we see that

$$\beta = a_1. \tag{24}$$

Substituting these results in Eq. 20, we have for $\phi_{ee}(\tau)$

$$\phi_{ee}(\tau) = \phi_{xx}(\tau) + \sum_{m=0}^{\infty} a_m^2 \phi_{xx}^m(\tau) - 2a_1\phi_{xx}(\tau), \tag{25}$$

since $\phi_{xx}(\tau) = \phi_{xx}(-\tau)$. After collecting terms, (25) becomes

$$\phi_{ee}(\tau) = a_o^2 + (1-a_1)^2\phi_{xx}(\tau) + \sum_{m=2}^{\infty} a_m^2\phi_{xx}^m(\tau). \tag{26}$$

Applying the Wiener theorem, we have for the power density spectrum of the quantizatinn error

$$\Phi_{ee}(\omega) = a_o^2 u_o(\omega) + (1-a_1)^2 \Phi_{xx}(\omega) + \sum_{m=2}^{\infty} a_m^2 \Phi_{xx}^{*m}(\omega). \tag{27}$$

It should be noted that the parameters denoted by a_m m = 0, 1, 2, ... in the expressions for the output and error autocorrelation functions and power density spectrum contain all the information concerning the specification of the quantizer. Further, the a_m are not functions of the autocorrelation function of the input signal. Thus, the a_m can be regarded as a set of parameters characterizing the quantizer from the autocorrelation or power-density points of view.

J. D. Bruce

References

1. J. D. Bruce, Optimum Quantization, Technical Report 429, Research Laboratory of Electronics, M. I. T. (in press).

2. J. D. Bruce, An Investigation of Optimum Quantization, Sc. D. Thesis, Department of Electrical Engineering, M. I. T., June 1964.

3. Y. W. Lee, Statistical Theory of Communication (John Wiley and Sons, Inc., New York, 1960), p. 51.

4. Ibid., pp. 209-213.

5. Ibid., p. 144.

6. D. Middleton, Introduction to Statistical Communication Theory (McGraw-Hill Book Company, Inc., New York, 1960), p. 337.

7. H. Cramér, Mathematical Methods of Statistics (Princeton University Press, Princeton, N. J., 1946), p. 133.

8. Y. W. Lee, op. cit., p. 56.

9. Ibid., p. 75.

10. J. J. Bussgang, Crosscorrelation Function of Amplitude-Distorted Gaussian Signals, Technical Report 216, Research Laboratory of Electronics, M. I. T., March 26, 1952.

E. AN APPLICATION OF VOLTERRA FUNCTIONAL ANALYSIS TO SHUNT-WOUND COMMUTATOR MACHINES

This report presents a solution to the nonlinear differential equations of a voltage-excited, shunt-wound commutator machine by an application of Volterra functional analysis. A Volterra series expression for the output speed of this machine, in terms of its input voltage, is derived. For a class of bounded inputs, the convergence of this series is proved. Bounds are given on the errors introduced if the higher order terms of this series are neglected.

1. Model of a Shunt-Wound Commutator Machine

Figure XVII-24 is a schematic model of a system that consists of a voltage-excited,

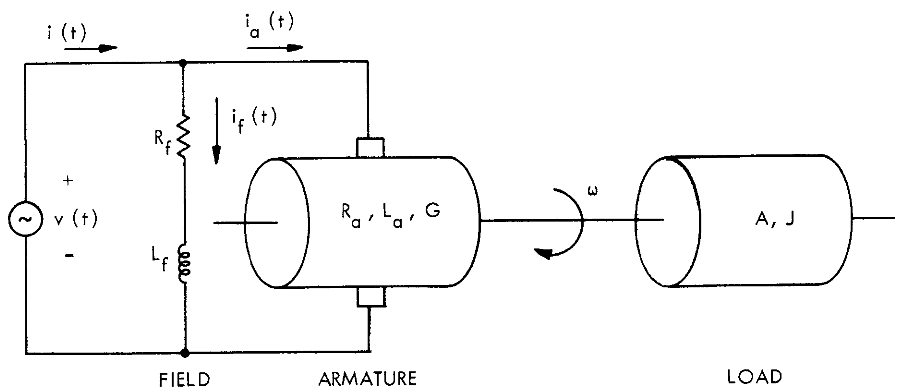

Fig. XVII-24. Voltage-excited shunt-wound commutator machine driving an inertial and frictional load.

shunt-wound, commutator machine and its load. The load is inertial and frictional. The parameters of this system[1] are:

- $v(t)$, excitation voltage (input)
- $\omega(t)$, rotation speed of the machine (output)
- $i_a(t)$, armature current
- $i_f(t)$, field current
- R_a, series resistance of the armature and brushes
- R_f, resistance of the field
- L_a, self-inductance of the armature
- L_f, self-inductance of the field
- G, speed coefficient of the machine
- A, load coefficient of torque drag per rotation speed
- J, moment of inertia of the load.

It will be assumed that R_a, R_f, L_a, L_f, G, A, and J are constants (that is, coil saturation and/or variable loading will not be considered). With these restrictions, the system's equations of motion[2] are:

$$v(t) = \left(R_f + L_f \frac{d}{dt}\right) i_f(t) \tag{1}$$

$$v(t) = \left(R_a + L_a \frac{d}{dt}\right) i_a(t) + G\omega(t)\, i_f(t) \tag{2}$$

$$G i_a(t)\, i_f(f) = \left(A + J \frac{d}{dt}\right) \omega(t). \tag{3}$$

For a given input, $v(t)$, Eqs. 1-3 is a set of three simultaneous equations in three unknowns $i_f(t)$, $i_a(t)$, and $\omega(t)$. As a first step toward solving these equations, Eqs. 1 and 2 will be solved for $i_f(t)$ and $i_a(t)$ in terms of $v(t)$ and $\omega(t)$. These results will then be used to eliminate these variables from Eq. 3 in order to obtain one equation in one unknown. The last equation in input and output will then be used to find a Volterra series solution for $\omega(t)$ in terms of $v(t)$.

2. Input-Output Equation

Equation 1 is linear and may be solved by standard techniques. The explicit solution for $i_f(t)$ in terms of $v(t)$ is

$$i_f(t) = \int_{-\infty}^{\infty} h_f(\tau)\, v(t-\tau)\, d\tau, \tag{4}$$

where

$$h_f(\tau) = \mu(\tau) \frac{1}{L_f} \exp\left[-\frac{R_f}{L_f}\tau\right], \tag{5}$$

and $\mu(\tau)$ is the unit step.

Equation 2 is nonlinear because of the $\omega(t)\, i_f(t)$ product. If $[v(t) - G\omega(t)\, i_f(t)]$ is treated as if it were one variable, then Eq. 2 is linear and can be solved for $i_a(t)$ in terms of the variable

$$i_a(t) = \int_{-\infty}^{\infty} h_a(\tau)[v(t-\tau) - G\omega(t-\tau)\, i_f(t-\tau)]\, d\tau, \tag{6}$$

where

$$h_a(\tau) = \mu(\tau) \frac{1}{L_a} \exp\left[-\frac{R_a}{L_a}\tau\right]. \tag{7}$$

The dependence in Eq. 6 of $i_a(t)$ upon $i_f(t)$ can be eliminated by substituting the expression for $i_f(t)$ given by Eq. 4. The result is

$$i_a(t) = \int_{-\infty}^{\infty} h_a(\tau_1)\, v(t-\tau_1)\, d\tau_1 - G \int_{-\infty}^{\infty}\int h_f(\tau_1)\, h_a(\tau_2)\, v(t-\tau_1-\tau_2)\, \omega(t-\tau_2)\, d\tau_1 d\tau_2. \tag{8}$$

If $[i_a(t)\, i_f(t)]$ is treated as if it were one variable, then Eq. 3 is linear and can be solved for $\omega(t)$ in terms of this variable. The result is

$$\omega(t) = \int_{-\infty}^{\infty} h_{\omega}(\tau)[i_a(t-\tau)\, i_f(t-\tau)]\, d\tau, \tag{9}$$

where

$$h_{\omega}(\tau) = \mu(\tau)\frac{G}{J}\exp\left[-\frac{A}{J}\tau\right]. \tag{10}$$

If the expressions for $i_f(t)$ and $i_a(t)$ given by Eqs. 4 and 8 are used to eliminate these variables from Eq. 9, the result is an equation in only the input, $v(t)$, and the output, $\omega(t)$. That input-output equation is

$$\begin{aligned}\omega(t) = & \int \underset{-\infty}{\overset{\infty}{\cdots}} \int h_f(\tau_1)\, h_a(\tau_2)\, h_{\omega}(\tau_3)\, v(t-\tau_1-\tau_3)\, v(t-\tau_2-\tau_3)\, d\tau_1 \dots d\tau_3 \\ & - G\int \underset{-\infty}{\overset{\infty}{\cdots}} \int h_f(\tau_1)\, h_a(\tau_2)\, h_f(\tau_3)\, h_{\omega}(\tau_4)\, v(t-\tau_1-\tau_2-\tau_4)\, v(t-\tau_3-\tau_4) \\ & \cdot \omega(t-\tau_2-\tau_4)\, d\tau_1 \dots d\tau_4 \end{aligned} \tag{11}$$

If the input $v(t)$ is bounded,

$$|v(t)| < \frac{R_f}{G}\sqrt{AR_a}, \text{ for all } t, \tag{12}$$

then the solutions of Eq. 11 are unique and time-invariant.

3. Output Speed as a Functional of the Input Voltage

If the output, $\omega(t)$, is an analytical functional of the input, $v(t)$, (that is, its Volterra series representation converges), then because it is time-invariant[3] we may write:

$$\omega(t) = \Omega_o + \sum_{n=1}^{\infty} \int \underset{-\infty}{\overset{\infty}{\cdots}} \int \Omega_n(\tau_1,\dots,\tau_n)\, v(t-\tau_1) \dots v(t-\tau_n)\, d\tau_1 \dots d\tau_n, \tag{14}$$

where Ω_o is a constant, and $\Omega_n(\tau_1,\dots,\tau_n)$ is a function of n variables.

In order to evaluate the Volterra kernels, Ω_o, Ω_1, ..., we substitute Eq. 14 in Eq. 11. With an appropriate change of dummy variables, the result is

$$\begin{aligned}\Omega_o + \sum_{n=1}^{\infty} \int \underset{-\infty}{\overset{\infty}{\cdots}} \int \Omega_n(\tau_1,\dots,\tau_n)\, v(t-\tau_1) \dots v(t-\tau_n)\, d\tau_1 \dots d\tau_n = \int_{-\infty}^{\infty}\int \Bigg\{\int_{-\infty}^{\infty} h_{\omega}(\zeta_1) \\ \cdot h_f(\tau_1-\zeta_1)\, h_a(\tau_2-\zeta_1)\, d\zeta_1 - G\Omega_o \int_{-\infty}^{\infty}\int h_a(\zeta_1)\, h_{\omega}(\zeta_2)\, h_f(\tau_1-\zeta_1-\zeta_2)\, h_f(\tau_2-\zeta_2)\, d\zeta_1 d\zeta_2\Bigg\}\end{aligned}$$

$$\cdot\, v(t-\tau_1)\, v(t-\tau_2)\, d\tau_1 d\tau_2 + \sum_{m=3}^{\infty} \int_{-\infty}^{\infty}\!\!\cdots\!\int \left\{ -G \int_{-\infty}^{\infty}\!\!\int h_a(\zeta_1)\, h_\omega(\zeta_2)\, h_f(\tau_{m-1}-\zeta_1-\zeta_2)\, h_f(\tau_m-\tau_2) \right.$$

$$\left. \cdot\, \Omega_{m-2}(\tau_1-\zeta_1-\zeta_2, \ldots, \tau_{m-2}-\zeta_1-\zeta_2)\, d\zeta_1 \zeta d_2 \right\} v(t-\tau_1) \ldots v(t-\tau_m)\, d\tau_1 \ldots d\tau_m. \qquad (15)$$

Equation 15 must hold for all v(t) for which the Volterra series, Eq. 14, converges. This can be true if and only if like order integrations of v(t) on either side of Eq. 15 are equal. That is,

$$\Omega_o = 0 \qquad (16)$$

$$\int_{-\infty}^{\infty} \Omega_1(\tau_1)\, v(t-\tau_1)\, d\tau_1 = 0 \qquad (17)$$

$$\int_{-\infty}^{\infty}\!\!\int \Omega_2(\tau_1, \tau_2)\, v(t-\tau_1)\, v(t-\tau_2)\, d\tau_1 d\tau_2 = \int_{-\infty}^{\infty}\!\!\int \left\{ \int_{-\infty}^{\infty} h_\omega(\zeta_1)\, h_f(\tau_1-\zeta_1)\, h_a(\tau_2-\zeta_1)\, d\zeta_1 \right\} \cdot v(t-\tau_1)\, v(t-\tau_2)\, d\tau_1 d\tau_2 \qquad (18)$$

$$\int_{-\infty}^{\infty}\!\!\int \Omega_n(\tau_1, \ldots, \tau_n)\, v(t-\tau_1) \ldots v(t-\tau_n)\, d\tau_1 \ldots d\tau_n = \int_{-\infty}^{\infty}\!\!\int \left\{ -G \int_{-\infty}^{\infty}\!\!\int h_a(\zeta_1)\, h_\omega(\zeta_2) \right.$$

$$\left. h_f(\tau_{n-1}-\zeta_1-\zeta_2)\, h_f(\tau_n-\zeta_2)\, \Omega_{n-2}(\tau_1-\zeta_1-\zeta_2, \ldots, \tau_{n-2}-\zeta_1-\zeta_2)\, d\zeta_1 d\zeta_2 \right\}$$

$$v(t-\tau_1) \ldots v(t-\tau_n)\, d\tau_1 \ldots d\tau_n \qquad \text{for } n \geq 3. \qquad (19)$$

Note that there is no second term on the right side of Eq. 18. This is because $\Omega_o = 0$ (Eq. 16).

At this point, we can deduce solutions for the kernels. We require the kernels to be piecewise continuous, and shall express them in symmetric form. Let us define

$$g(a, \beta) = \int_{-\infty}^{\infty} h_\omega(\zeta)\, h_f(a-\zeta)\, h_a(\beta-\zeta)\, d\zeta. \qquad (20)$$

The solutions are

$$\Omega_o = 0 \qquad (21)$$

$$\Omega_1(\tau_1) = 0 \qquad (22)$$

$$\Omega_2(\tau_1, \tau_2) = \frac{1}{2} g(\tau_1, \tau_2) + \frac{1}{2} g(\tau_2, \tau_1) \qquad (23)$$

$$\Omega_n(\tau_1,\ldots,\tau_n) = \underset{(\tau_1,\ldots,\tau_n)}{\text{Sym}}\left\{-G\int_{-\infty}^{\infty}\int h_a(\zeta_1)\,h_\omega(\zeta_2)\,h_f(\tau_{n-1}-\zeta_1-\zeta_2)\,h_f(\tau_n-\zeta_2)\right.$$

$$\left.\cdot\,\Omega_{n-2}(\tau_1-\zeta_1-\zeta_2,\ldots,\tau_{n-2}-\zeta_1-\zeta_2)\,d\zeta_1 d\zeta_2\right\}; \qquad \text{for } n \geq 3, \tag{24}$$

where

$$\underset{(\tau_1,\ldots,\tau_n)}{\text{Sym}}\left\{f(\tau_1,\ldots,\tau_n)\right\}$$

indicates the operation of symmetrization[4] of the function $f(\ldots)$ in its arguments; τ_1, $\ldots$, τ_n. This is accomplished by summing $f(\ldots)$ in all $n!$ possible permutations of its τ's and dividing the result by $n!$

4. Evaluation of the First Nonzero Kernel

As a first step toward evaluating $\Omega_2(\tau_1,\tau_2)$ by Eq. 23, let us evaluate $g(\alpha,\beta)$. When the expressions for $h_f(\tau)$, $h_a(\tau)$, and $h_\omega(\tau)$, given by Eqs. 5, 7, and 10, are substituted in Eq. 20, the result is

$$g(\alpha,\beta) = \int_{-\infty}^{\infty} \mu(\zeta)\,\mu(\alpha-\zeta)\,\mu(\beta-\zeta)\,\frac{G}{JL_fL_a}\,e^{-\left(\frac{R_f}{L_f}\alpha+\frac{R_a}{L_a}\beta\right)+\left(\frac{R_f}{L_f}+\frac{R_a}{L_a}-\frac{A}{J}\right)\zeta}\,d\zeta$$

$$= \mu(\alpha)\,\mu(\beta)\,\frac{G}{JL_fL_a}\,e^{-\left(\frac{R_f}{L_f}\alpha+\frac{R_a}{L_a}\beta\right)}\int_0^{\underline{m}(\alpha,\beta)} e^{+\left(\frac{R_f}{L_f}+\frac{R_a}{L_a}-\frac{A}{J}\right)\zeta}\,d\zeta \tag{25}$$

Here, $\underline{m}(\alpha,\beta)$ is the minimum of α and β:

$$\underline{m}(\alpha,\beta) = \left\{\begin{matrix}\alpha, & \alpha\leq\beta \\ \beta, & \alpha\geq\beta\end{matrix}\right\}. \tag{26}$$

When the integration indicated in Eq. 25 is performed, the result is

$$\mu(\alpha)\,\mu(\beta)\,\frac{G}{JL_fL_a}\,e^{-\left(\frac{R_f}{L_f}\alpha+\frac{R_a}{L_a}\beta\right)}\,\frac{e^{+\left(\frac{R_f}{L_f}+\frac{R_a}{L_a}-\frac{A}{J}\;\underline{m}(\alpha,\beta)\right)}-1}{\frac{R_f}{L_f}+\frac{R_a}{L_a}-\frac{A}{J}}$$

for the case $\frac{R_f}{L_f}+\frac{R_a}{L_a}\neq\frac{A}{J}$, and

$$g(\alpha, \beta) \doteq \mu(\alpha)\,\mu(\beta)\,\frac{G}{JL_fL_a}\,e^{-\left(\frac{R_f}{L_f}\alpha+\frac{R_a}{L_a}\beta\right)}\,\underline{m}(\alpha, \beta) \tag{27}$$

for the case $\frac{R_f}{L_f} + \frac{R_a}{L_a} = \frac{A}{J}$.

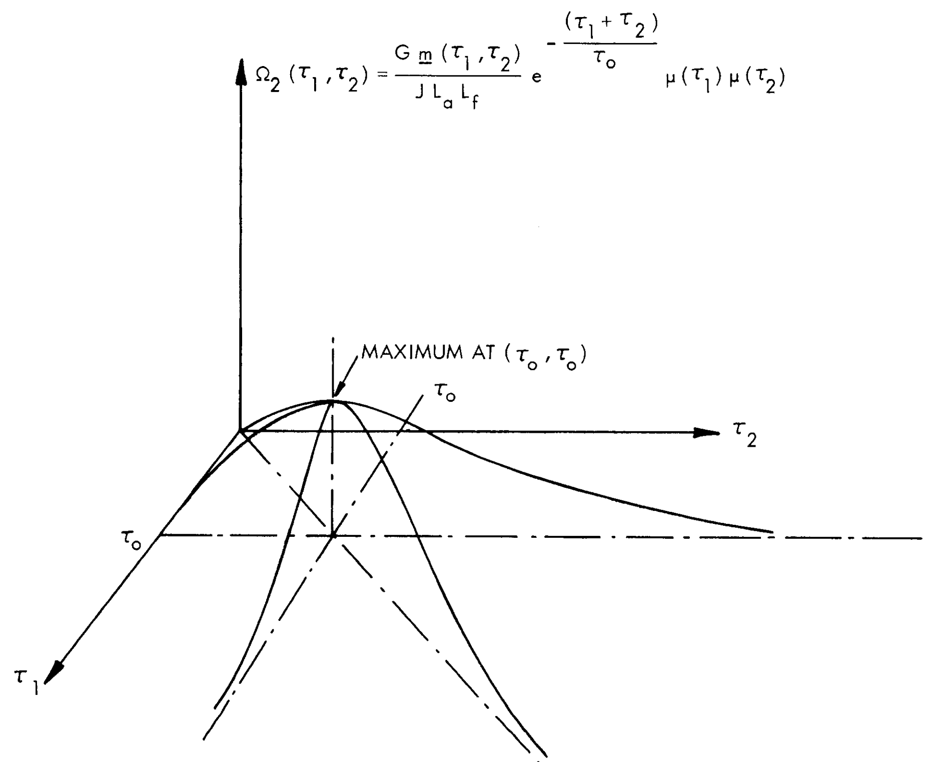

Fig. XVII-25. The second-order kernel for the special case.

The first nonzero kernel $\Omega_2(\tau_1, \tau_2)$ is now found by symmetrizing Eq. 27 (see Eq. 23). The result is stated below. Figure XVII-2 shows $\Omega_2(\tau_1, \tau_2)$ for the special case

$$\frac{R_a}{L_f} = \frac{R_a}{L_a} = \frac{A}{2J} = \frac{1}{\tau_o}. \tag{28}$$

For the case $\frac{R_f}{L_f} + \frac{R_a}{L_a} \neq \frac{A}{J}$:

$$\Omega_2(\tau_1,\tau_2) = \mu(\tau_1)\,\mu(\tau_2)\,\frac{G}{2(JL_aR_f+JL_fR_a-L_aL_fA)}$$
$$\cdot\left\{\exp\left[-\left(\frac{R_f}{L_f}\tau_1+\frac{R_a}{L_a}\tau_2\right)\right]+\exp\left[-\left(\frac{R_a}{L_a}\tau_1+\frac{R_f}{L_f}\tau_2\right)\right]\right\}$$
$$\cdot\left\{\exp\left[+\left(\frac{R_f}{L_f}+\frac{R_a}{L_a}-\frac{A}{J}\right)\underline{m}(\tau_1,\tau_2)\right]-1\right\}.$$

For the case $\frac{R_f}{L_f}+\frac{R_a}{L_a}=\frac{A}{J}$:

$$\Omega_2(\tau_1,\tau_2) = \mu(\tau_1)\,\mu(\tau_2)\,\frac{G\underline{m}(\tau_1,\tau_2)}{2JL_aL_f}$$
$$\cdot\left\{\exp\left[-\left(\frac{R_f}{L_f}\tau_1+\frac{R_a}{L_a}\tau_2\right)\right]+\exp\left[-\left(\frac{R_a}{L_a}\tau_1+\frac{R_f}{L_f}\tau_2\right)\right]\right\}.$$

5. Evaluation of the Higher Order Kernels

Equation 24 is a recursion formula whereby each of the higher order kernels ($\Omega_3,\Omega_4,\Omega_5,\ldots$) can be evaluated by an integral and symmetrization operation upon that kernel which precedes it by two orders. Since Eq. 22 states that Ω_1 is zero, it then follows that Ω_3, Ω_5, Ω_7, ...; all of the succeeding odd-order kernels are zero.

$$\Omega_{2m+1}(\tau_1,\ldots,\tau_{2m+1}) = 0, \qquad \text{for } m = 0, 1, 2, \ldots \tag{29}$$

The even-order kernels, except for Ω_o, do not vanish. Indeed, it can be shown that

$$\left\{\begin{array}{ll} (-)^{m+1}\Omega_{2m}(\tau_1,\ldots,\tau_{2m}) > 0; & \text{if each of } \tau_1, \ldots, \tau_{2m} > 0 \\ \Omega_{2m}(\tau_1,\ldots,\tau_{2m}) = 0; & \text{if any of } \tau_1, \ldots, \tau_{2m} \leqslant 0 \end{array}\right\}$$
$$\text{for } m = 1, 2, 3, \ldots. \tag{30}$$

These results allow us to rewrite the Volterra series representation for the speed functional in a more convenient form. That is, if the series at Eq. 14 converges, then by Eqs. 21, 29, and 30 we may write:

$$\omega(t) = \sum_{m=1}^{\infty} \int \overset{\infty}{\underset{-\infty}{\cdots}} \int \Omega_{2m}(\tau_1,\ldots,\tau_{2m})\, v(t-\tau_1)\ldots v(t-\tau_{2m})\, d\tau_1 \ldots d\tau_{2m}. \tag{31}$$

Two results follow immediately from Eq. 31. First, $\omega(t)$ is an even function of $v(t)$. That is, if

$$v(t) \longrightarrow \omega(t),$$

then

$$-v(t) \longrightarrow \omega(t). \tag{32}$$

Second, the speed functional is realizable. That is,

$$\omega(t) \text{ is independent of } v(t'), \text{ for all } t' > t. \tag{33}$$

6. Demonstration of Convergence

We may now prove that the Volterra series representation of the speed functional converges absolutely for a class of bounded inputs:

$$|v(t)| \leqslant V, \qquad \text{for all } t. \tag{34}$$

Consider the absolute value of the output speed, $\omega(t)$. By Eqs. 31 and 34,

$$|\omega(t)| \leqslant \sum_{m=1} \int_0^\infty \cdots \int V^{2m} |\Omega_{2m}(\tau_1, \ldots, \tau_{2m})| \, d\tau_1 \ldots d\tau_{2m}, \qquad \text{for all } t. \tag{35}$$

It can be shown that

$$\int_0^\infty \cdots \int |\Omega_{2m}(\tau_1, \ldots, \tau_{2m})| \, d\tau_1 \ldots d\tau_{2m} = \left(\frac{R_f}{G}\right)\left(\frac{G^2}{AR_aR_f^2}\right)^m \qquad \text{for } m = 1, 2, 3, \ldots. \tag{36}$$

When the expression for the integral of the absolute value of the $2m^{th}$ kernel, Eq. 36, is substituted in Eq. 35, the resultant power series converges to

$$|\omega(t)| \leqslant \frac{R_fGV^2}{AR_aR_f^2 - G^2V^2}, \qquad \text{for all } t \tag{37}$$

whenever

$$\frac{G^2V^2}{AR_aR_f^2} < 1. \tag{38}$$

Thus it has been shown, by Eqs. 34, 37, and 38, that the Volterra series representation of the speed functional, either Eqs. 14 or 31, converges absolutely whenever the input voltage, $v(t)$, is bounded in such a way that

$$|v(t)| \leq V < V_B = \frac{R_f\sqrt{AR_a}}{G}, \qquad \text{for all } t. \tag{39}$$

It should be noted that while Eq. 39 is a sufficient condition for convergence, it is not a necessary condition.

Since, for the class of input voltages specified by Eq. 39, the Volterra series speed functional, Eq. 31, converges, and this series satisfies Eq. 11 by construction, and, for this class of inputs, the solutions of Eq. 11 are unique, it is proved that $\omega(t)$, as given by Eq. 31, is the output speed of this shunt-wound commutator machine for any arbitrary input voltage, $v(t)$, that satisfies Eq. 39.

A literature search has failed to uncover any other published solution of the output speed of a shunt commutator machine for an arbitrary input voltage.[5,6]

7. Errors of Truncation

If the Volterra series for $\omega(t)$ is approximated by its first N nonzero terms and higher order terms are neglected,

$$\omega_N(t) = \sum_{n=1}^{N} \int_0^\infty \cdots \int \Omega_{2n}(\tau_1, \ldots, \tau_{2n})\, v(t-\tau_1) \ldots v(t-\tau_{2n})\, d\tau_1 \ldots d\tau_{2n}, \tag{40}$$

where N is an integer ≥ 1, then the truncation error of the approximation is

$$\epsilon_N(t) = \omega(t) - \omega_N(t). \tag{41}$$

If the input voltage, $v(t)$, satisfies Eq. 39, then by the use of Eqs. 31, 40, and 41, it follows that the absolute value of the truncation error is bounded

$$|\epsilon_N(t)| \leq \sum_{n=N+1} \int_0^\infty \cdots \int V^{2n} |\Omega_{2n}(\tau_1, \ldots, \tau_{2n})|\, d\tau_1 \ldots d\tau_{2n}, \qquad \text{for all } t. \tag{42}$$

When the expression for the integral of the absolute value of the $2n^{th}$ kernel, Eq. 36, is substituted in Eq. 42, the resultant power series converges and, with the definition of V_B introduced in Eq. 39, the sum of that power series is

$$|\epsilon_{N(t)}| \leq \frac{R_f}{G} \frac{\left(\frac{V}{V_B}\right)^{2(N+1)}}{1 - \left(\frac{V}{V_B}\right)^2}, \qquad \text{for all } t. \tag{43}$$

R. B. Parente

References

1. D. C. White and H. H. Woodson, Electromechanical Energy Conversion (John Wiley and Sons, Inc., New York, 1959), p. 278.

2. Ibid., p. 280; see Eq. 4-57.

3. V. Volterra, Theory of Functionals and of Integral and Integro-Differential Equations (Dover Publications, Inc., New York, reprint 1959), p. 21.

4. N. Wiener, Nonlinear Problems in Random Theory (John Wiley and Sons, Inc., New York, 1958), pp. 17-18.

5. IEEE Committee Report, Bibliography of Rotating Electric Machinery for 1948-1961, IEEE Trans. Power Apparatus and Systems, Vol. 83, No. 6, pp. 589-606, June 1964.

6. AIEE Publication S-32, Bibliography of Rotating Electric Machinery, 1886-1947 (American Institute of Electrical Engineers, n. d.).